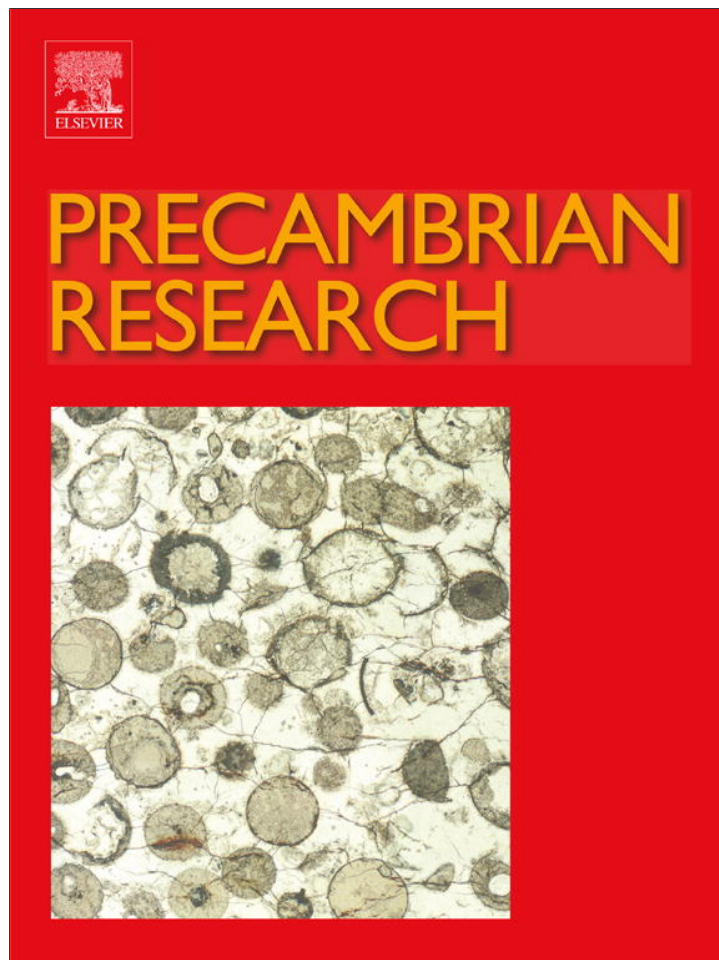


Provided for non-commercial research and education use.
Not for reproduction, distribution or commercial use.



This article appeared in a journal published by Elsevier. The attached copy is furnished to the author for internal non-commercial research and education use, including for instruction at the authors institution and sharing with colleagues.

Other uses, including reproduction and distribution, or selling or licensing copies, or posting to personal, institutional or third party websites are prohibited.

In most cases authors are permitted to post their version of the article (e.g. in Word or Tex form) to their personal website or institutional repository. Authors requiring further information regarding Elsevier's archiving and manuscript policies are encouraged to visit:

<http://www.elsevier.com/authorsrights>



Contents lists available at SciVerse ScienceDirect

Precambrian Research

journal homepage: www.elsevier.com/locate/precamres

Problematic urn-shaped fossils from a Paleoproterozoic (2.2 Ga) paleosol in South Africa



Gregory J. Retallack^{a,*}, Evelyn S. Krull^b, Glenn D. Thackray^c, Dula Parkinson^d

^a Department of Geological Sciences, University of Oregon, Eugene, OR 97403, United States

^b C.S.I.R.O. Land and Water, Waite Campus, Glen Osmond, South Australia 5064, Australia

^c Department of Geosciences, Idaho State University, Pocatello, ID 83209, United States

^d Lawrence Berkeley National Laboratory, 1 Cyclotron Road, Berkeley, CA 94720, United States

ARTICLE INFO

Article history:

Received 16 January 2013

Received in revised form 22 May 2013

Accepted 23 May 2013

Available online xxx

Keywords:

Paleosol

Lichen

South Africa

Paleoproterozoic

Hekpoort Basalt

ABSTRACT

Small (0.3–1.8 mm long), locally abundant, urn-shaped fossils within surface horizons of a paleosol in the 2.2 Ga Hekpoort Formation near Waterval Onder, South Africa, are here described and named *Diskagma buttonii* Retallack gen. et sp. nov. The fossils are from fresh rock of a deep highway cutting, and have been metamorphosed to upper greenschist facies like their matrix. Despite metamorphic alteration, total organic carbon of the samples was 0.04% and its isotopic composition ($\delta^{13}\text{C}$) was $-25.6 \pm 0.08\%$ (two standard deviations) versus Vienna Pee Dee belemnite standard. Organic outlines of the fossils are also accentuated by recrystallized berthierine and opaque oxides. The fossils are locally clumped within surface swales of a Vertisol paleosol, identified from characteristic penecontemporaneous deformation (clastic dikes between swales of mukgara structure) and from pronounced geochemical differentiation (phosphorus and copper strain-corrected mass-depletion characteristic of an oxidized biologically active soil). This paleosol's chemical composition is evidence of temperate humid climate (mean annual temperature $11.3 \pm 4.4^\circ\text{C}$, and mean annual precipitation 1489 ± 182 mm). Associated paleosols indicate atmospheric CO_2 of 6640 (+12,880/–4293) ppm (0.6%) and 0.9–5% atmospheric O_2 . The best preserved examples of *Diskagma* are shaped like an urn with a flared rim, and closed below the flare. Observation of hundreds of specimens in thin section reveals substantial variation in growth (elongation) and decay (shredding and deflation). They had a hollow ellipsoidal interior that is unusually devoid of opaque debris, unlike the matrix. *Diskagma* is superficially comparable with lichens such as *Cladonia* (Ascomycota) and *Geosiphon* (Glomeromycota). Definitive reproductive structures remain unknown. They predate the oldest other likely fossil eukaryotes (1.9 Ga) and fungi (1.5 Ga), and current molecular clock estimates for eukaryotes (1.6 Ga) and fungi (1.1 Ga). Lichenized actinobacteria are plausible prokaryotic alternatives permitted by molecular clocks. Although biological affinities of *Diskagma* are uncertain, these fossils reveal the general appearance of Paleoproterozoic life on land.

© 2013 Elsevier B.V. All rights reserved.

1. Introduction

Much is now known about Precambrian life in the ocean (Schopf and Klein, 1991; Knoll, 2003). Marine prokaryotic microfossils (Sugitani et al., 2009; Schopf et al., 2010; Wacey et al., 2011) and stromatolites (Allwood et al., 2006; van Kranendonk et al., 2008) are known as old as 3.5 Ga. Large marine organic fossils, such as the possible eukaryotic *Grypania spiralis*, are no older than 1.9 Ga (Han and Runnegar, 1992; Schneider et al., 2002). Large complex microfossils interpreted as eukaryotic marine plankton may be no older than 1.8 Ga (Lamb et al., 2009) and comparable lacustrine eukaryotes only 1.2 Ga (Strother et al., 2011). In contrast, evidence

for life on land is established as far back as 2.6–2.8 Ga, from paleosols with biogenic carbon isotopic compositions (Watanabe et al., 2004) and patterns of P, Fe and Cu depletions (Neaman et al., 2005). There also are puzzling large Archean organic structures in paleosols (Hallbauer and van Warmelo, 1974; Hallbauer et al., 1977; Mossman et al., 2008), although their biogenicity has been disputed (Cloud, 1976; Barghoorn, 1981). This study reports new problematica of comparable size, unusual complexity and Paleoproterozoic age, from the surface horizon of the Waterval Onder paleosol (2.2 Ga), in the uppermost Hekpoort Formation, near Waterval Onder, Transvaal, South Africa (Figs. 1–3; Table 1). These structures were first noted in thin section by Button (1979), but they are too large and their matrix insufficiently translucent to reveal three-dimensional shape in blocks thick enough to enclose them (Retallack and Krinsley, 1993). Here we present additional hand specimens and petrographic observations (Fig. 4), and

* Corresponding author. Tel.: +1 541 346 4558; fax: +1 541 346 4692.
E-mail address: gregr@uoregon.edu (G.J. Retallack).

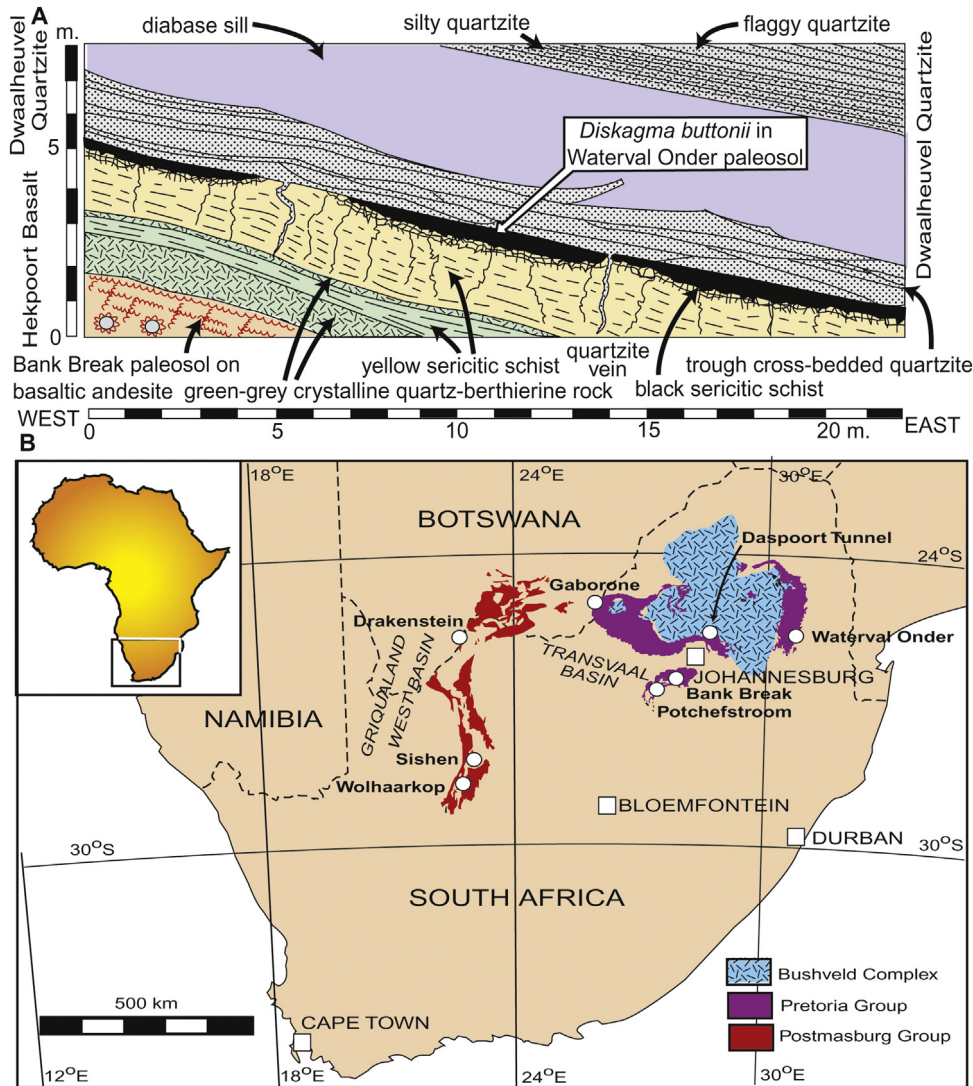


Fig. 1. Fossil locality within surface horizon of Vertisol paleosol within the upper Hekpoort Basalt (2.2 Ga) in roadcut (A), near Waterval Onder, Transvaal Basin, South Africa (B).

synchrotron X-ray tomographic results (Fig. 5) for the three dimensional shape of these problematic structures of a Paleoproterozoic paleosol.

Three principal questions are addressed by this paper. Are these Waterval Onder paleosol problematic structures fossils? Are they comparable with other enigmatic structures from paleosols? What kind of organisms could they have been?

Table 1
Stratigraphy of the Pretoria Group, Transvaal Basin, South Africa.

Formation	Lithology	Paleoenvironment	Thickness (m)
Houtenbek Formation	Quartzite, carbonate and chert	Epeiric sea	140–225
Steenkampsberg Quartzite	Quartzite with minor shale	Epeiric sea coast	470–255
Niederhorst Formation	Argillaceous quartzite, and arkose	Epeiric sea	200–800
Lakenvalei Quartzite	Quartzite and arkose	Epeiric sea coast	160–300
Vermont Hornfels	Hornfels, quartzite, dolomite, and chert	Epeiric sea	450–800
Magaliesberg Quartzite	Quartzite with minor shale	Epeiric sea coast	500
Silverton Shale	Shale with minor chert and dolomite	Epeiric sea	1000–3300
Daspoort Quartzite	Quartzite with some shale	Alluvial marine in east	5–90
Strubenkop Shale	Shale with minor quartzite	Lacustrine	20–80
Dwaalheuvel Quartzite	Quartzite, with red siltstone and conglomerate	Alluvial	40–110
Hekpoort Formation	Andesite, with pyroclastics, quartzite and shale	Suberial volcanics, paleosols	0–500
Boshoek Formation	Quartzite, with siltstone and conglomerate	Alluvial	0–90
Timeball hill Formation	Quartzite, with shale and diamictite	Epeiric sea	900–1600
Rooihoogte Formation	Quartzite, with breccia	Alluvial and lacustrine	0–50

Note: From Kent (1980), Bekker et al. (2005), and Oberholzer and Eriksson (2000).

2. Materials and methods

Three-dimensional structure of problematic structures from the Waterval Onder paleosol was resolved by X-ray microtomography using the Lawrence Berkeley National Laboratory, Advanced Light Source (synchrotron), beam line 8.3.2. Because of the opacity of the matrix, beam energy was 45 keV, and samples needed to be

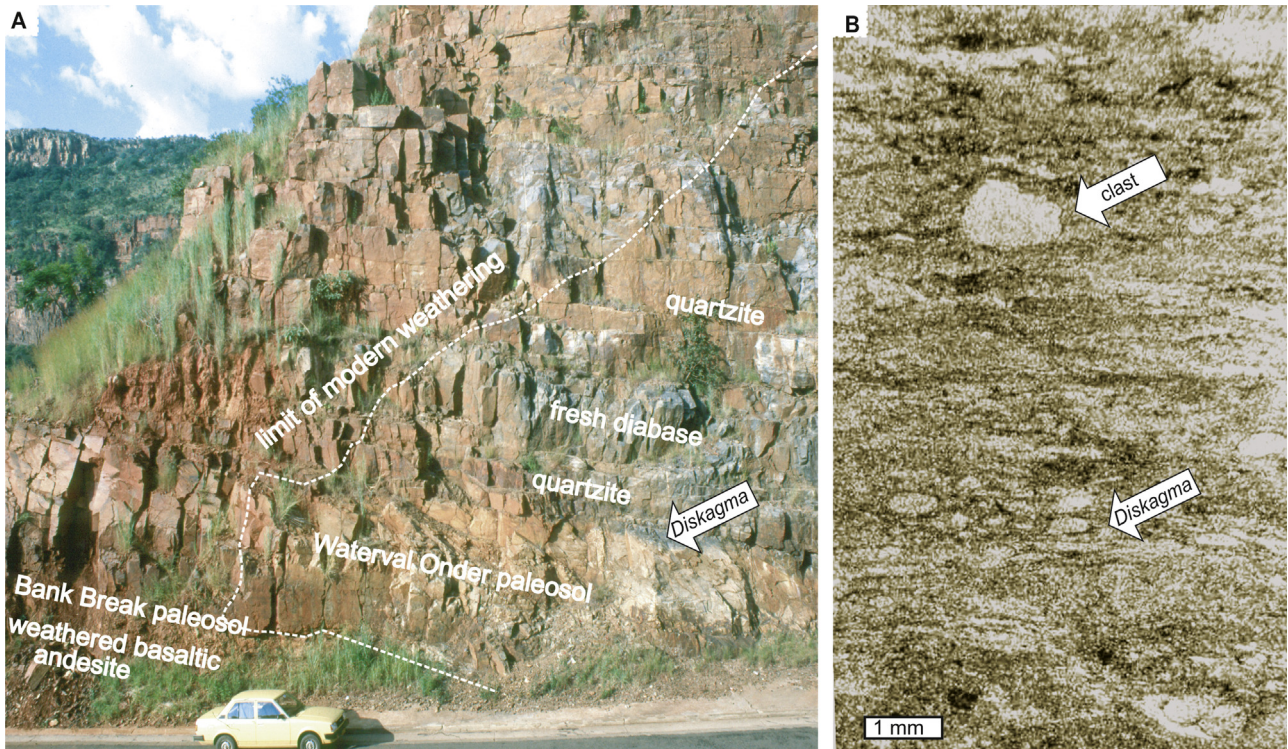


Fig. 2. Overview of deep roadcut near Waterval Onder, showing depth of surface (Miocene?) weathering (A), and clasts and fossiliferous bands (with *Diskagma buttonii* Retallack gen et sp. nov.) in a vertically oriented thin section of the surface horizon of the Waterval Onder paleosol (B).

less than 3 mm in diameter to obtain resolution of 1.8 μm , which is the pixel size and also the slice thickness of successive tomographic images. Successive slices were visualized in the computer program Fiji, and three-dimensional rendering done with program Aviso 6.2 (by Parkinson). Videos of slice sequences and rotations of a three dimensional rendering are available as Inline Supplementary Material videos 1 and 2.

Supplementary material related to this article can be found, in the online version, at <http://dx.doi.org/10.1016/j.precamres.2013.05.015>.

Geochemical characterization of the problematic structures reported here (by Thackray and Krull) included microprobe studies with a Cameca X50, in the Department of Geological Sciences, University of Oregon. Studies of carbon-coated polished thin sections enabled elemental mapping of Al, K, Si, Fe, Ti and Mn (Fig. 6), as well as back-scatter electron images in which brightness is correlated with elemental atomic number (Fig. 5K and L). Semiquantitative microprobe analyses for selected line transects of polished sections were also attempted (Fig. 7). Analyses of trace elements Cu, Cr, Zn, S and Cr and bulk density measurements were reported previously (Button, 1979; Retallack, 1986).

Seven specimens of the problematic structures in matrix were cut out with a diamond saw and each digested in 60% HF for 24 h, then analyzed for organic carbon content and isotopic composition by Bill Hagopian in the University of Hawaii laboratory of A. Hope Jahren by combustion in a Eurovector element analyzer (EURO.EA3000) and analysis in an Isoprime continuous-flow stable isotope mass spectrometer.

A variety of mathematical manipulations of these geochemical data were undertaken to determine degree of soil formation and soil-forming conditions of the enclosing paleosol. Soil formation involves both adjustments of volume from rock to soil (strain) as well as gains and losses of constituents (mass transfer). As recommended by Brimhall et al. (1992), changes in volume of soil during weathering were estimated from an immobile element in soil (such

as Ti used here) compared with parent material ($\epsilon_{i,w}$ as a fraction). The mass transfer of elements in a soil at a given horizon ($\tau_{j,w}$ in moles) was calculated from the bulk density of the soil (ρ_w in g cm^{-3}) and parent material (ρ_p in g cm^{-3}) and from the chemical concentration of the element in soils ($C_{j,w}$ in weight%) and parent material ($C_{j,p}$ in weight%). Eqs. (1) and (2) (below) are the basis for calculating divergence from parent material composition (assigned zero strain and mass transfer by definition):

$$\tau_{j,w} = \left[\frac{\rho_w \cdot C_{j,w}}{\rho_p \cdot C_{j,p}} \right] [\epsilon_{i,w} + 1] - 1 \quad (1)$$

$$\epsilon_{i,w} = \left[\frac{\rho_p \cdot C_{j,p}}{\rho_w \cdot C_{j,w}} \right] - 1 \quad (2)$$

Former temperature and precipitation can be inferred from chemical composition of paleosols. For example, the paleohyrometer of Sheldon et al. (2002), uses chemical index of alteration without potash ($R = 100\text{mAl}_2\text{O}_3 / (\text{mAl}_2\text{O}_3 + \text{mCaO} + \text{mNa}_2\text{O})$, in moles), which increases with mean annual precipitation (P in mm) in modern soils ($R^2 = 0.72$; S.E. = ± 182 mm), as follows:

$$P = 221e^{0.0197R} \quad (3)$$

This formulation is based on the hydrolysis equation of weathering, which enriches alumina at the expense of lime, magnesia, potash and soda. Magnesia is ignored because not significant for most sedimentary rocks, and potash is excluded because it can be enriched during deep burial alteration of sediments (Maynard, 1992).

A useful paleotemperature proxy for paleosols devised by Sheldon et al. (2002) uses alkali index ($N = (\text{K}_2\text{O} + \text{Na}_2\text{O}) / \text{Al}_2\text{O}_3$ as a molar ratio), which is related to mean annual temperature (T in $^\circ\text{C}$) in modern soils by Eq. (4) ($R^2 = 0.37$; S.E. = ± 4.4 $^\circ\text{C}$):

$$T = -18.5N + 17.3 \quad (4)$$

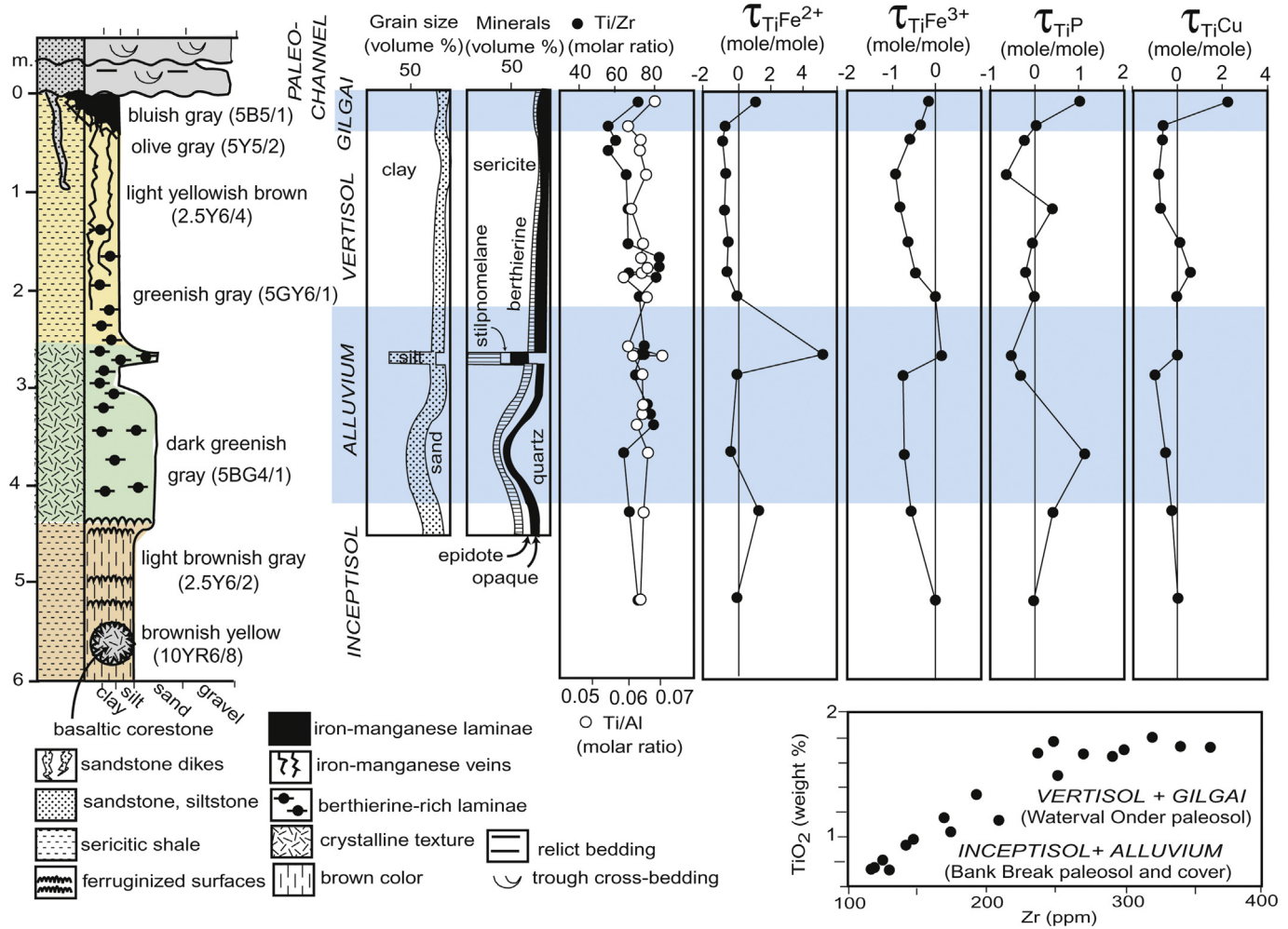


Fig. 3. Stratigraphic section and petrographic data on the Waterval Onder paleosol (Retallack, 1986). Selected geochemical data (after Button, 1979; Rye and Holland, 2000a) shows divergence of resistate elements (Ti, Zr) as evidence for different parent material zones and surface cumulus swales (gilgai) in the paleosol. Strain corrected mass transfer (following Brimhall et al., 1992) shows surficial losses of Fe²⁺, Fe³⁺, P and Cu as evidence for soil microbiota in a moderately oxygenated environment (Neaman et al., 2005).

The paleohyrometer and paleothermometer of Sheldon et al. (2002) have a training set of modern soils under vascular land plants, and may not prove appropriate for Precambrian paleosols. Such estimates can be regarded as heuristically useful until contradicted by more compelling alternative approaches.

Measurement of 153 specimens of the problematic fossils were made in 9 thin sections, including internal cavity length, internal cavity diameter, wall thickness, overall length, terminal cup diameter, terminal cup length, and short axis diameter coplanar and vertical to bedding. Measurements were made using gradations on an eyepiece micrometer and converted to mm by calibration with a stage scale. Density of the problematic structures was also measured in line transects parallel to bedding in thin section (Supplementary Inline Material Table S1). For comparison, 589 individuals of a single colony of the living lichen *Cladonia ecmocyna* were collected from the ridge east of the outlet to Fishtrap Lake, Sanders County, Montana, in June 7, 2008, and measurements made of podetia diameter and length, scyphus diameter and apothecia diameter using digital calipers. Tests for the normality and log-normality of size distributions were performed using the computer program JMP9.0 (Supplementary Inline Material Table S2).

Inline Supplementary Tables S1 and S2 can be found online at <http://dx.doi.org/10.1016/j.precamres.2013.05.015>.

Original soil thickness (D_s in m) can be reconstructed from paleosol thickness (D_p in m) after compaction during burial, and this

can be calculated from estimated thickness of overburden (K in km) using a standard compaction formula with physical constants for Vertisols (Sheldon and Retallack, 2001), as shown in Eq. (5). Comparable Eqs. (6) and (7), with different physical constants, for reconstructing log and jellyfish thickness (D_l in m) and possible fungal fossils (D_f) from fossils compacted by overburden (D_c in m) are derived from data of Retallack (2007).

$$D_s = \frac{-0.69D_p}{(0.31/e^{0.12K}) - 1} \quad (5)$$

$$D_f = \frac{-0.4D_c}{(0.6/e^{0.52K}) - 1} \quad (6)$$

$$D_l = \frac{-0.7D_c}{(0.9/e^{1.7K}) - 1} \quad (7)$$

3. Biogenicity criteria

Criteria for establishing the biogenicity of Precambrian problematica have been best articulated by Hans Hoffman (2004). The following text follows his six proposed tests, based on (1) known provenance, (2) plausible environment for life, (3) same age as the rock, (4) plausible composition (5) taphonomic series, and (6) repeated complexity.

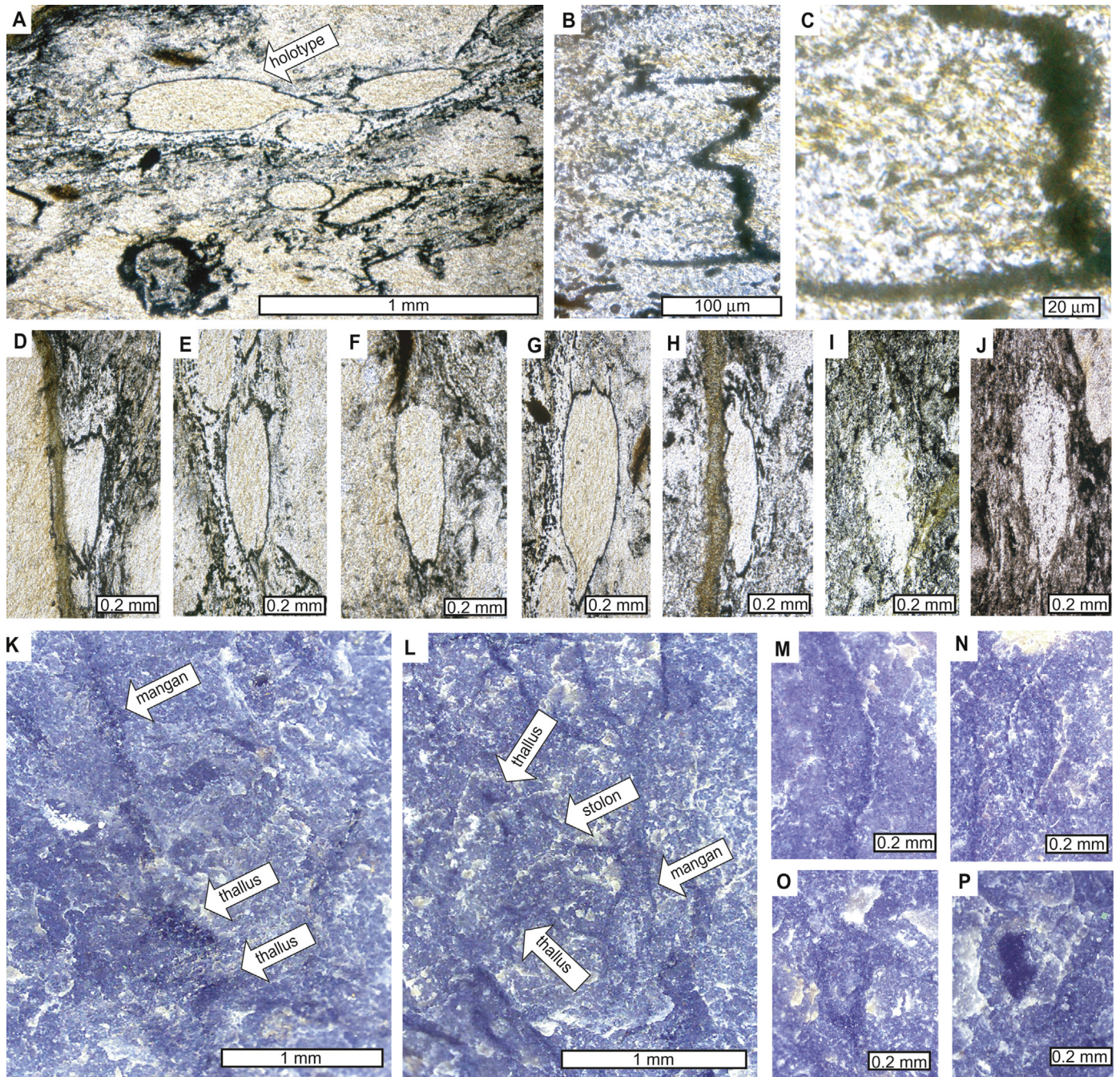


Fig. 4. *Diskagma buttoni* Retallack gen. et sp. nov. bedding plane exposure (K–P) and in petrographic thin sections (A–J) in natural orientation vertical to bedding (A–C) and depicted as if vertical for comparison, even when strata concordant (D–J): A–C, holotype specimen; D, specimen cut by metamorphic berthierine vein; D–J, natural variation in size and decay; K and L, iron–manganese-filled cracks (mangans), tubular organic structures (stolons) and thalli of *Diskagma*; M and P, individual thalli of *Diskagma* showing basal narrowing, irregular spine-like protrusions and longitudinal striation. Specimens are from thin section F116533A and hand specimen F116530A (Museum of Natural and Cultural History, University of Oregon).

3.1. Known provenance

The problematic structures considered here were collected in 1984 as part of a paleosol geochemical study (Retallack, 1986) from fresh rock 10 m below the land surface, and 4 m below the limit of modern oxidative weathering, in a deep road cut excavated in 1975 on national highway 4, 2.7 km east of Waterval Onder, Transvaal, South Africa (Figs. 1, 2A: S25.645330° E30.357676°). The fossils come from 10 to 25 cm below the contact between a paleosol forming the top of the Hekpoort Formation, and overlying trough cross-bedded sandstones of the Dwaalheuvél Quartzite,

within the lower Pretoria Group (Table 1). Comparable rounded grains of quartz are found in the Dwaalheuvél Quartzite and in clastic dikes reaching as much as 2 m down into the paleosol. These dikes are within mounds of yellow sericite, but the fossils are in a layered cumulic surface horizon of the paleosol above a distinctive breccia-like horizon (blocky peds) defined by iron–manganese veins (mangans). The diked mounds and flanking dark swales are characteristic mukgara structures of Vertisol paleosols (Retallack, 1986; Driese, 2004), and are evidence that the fossils were in seasonally inundated surface swales (gilgai microrelief) overlain by fluvial sandstone.

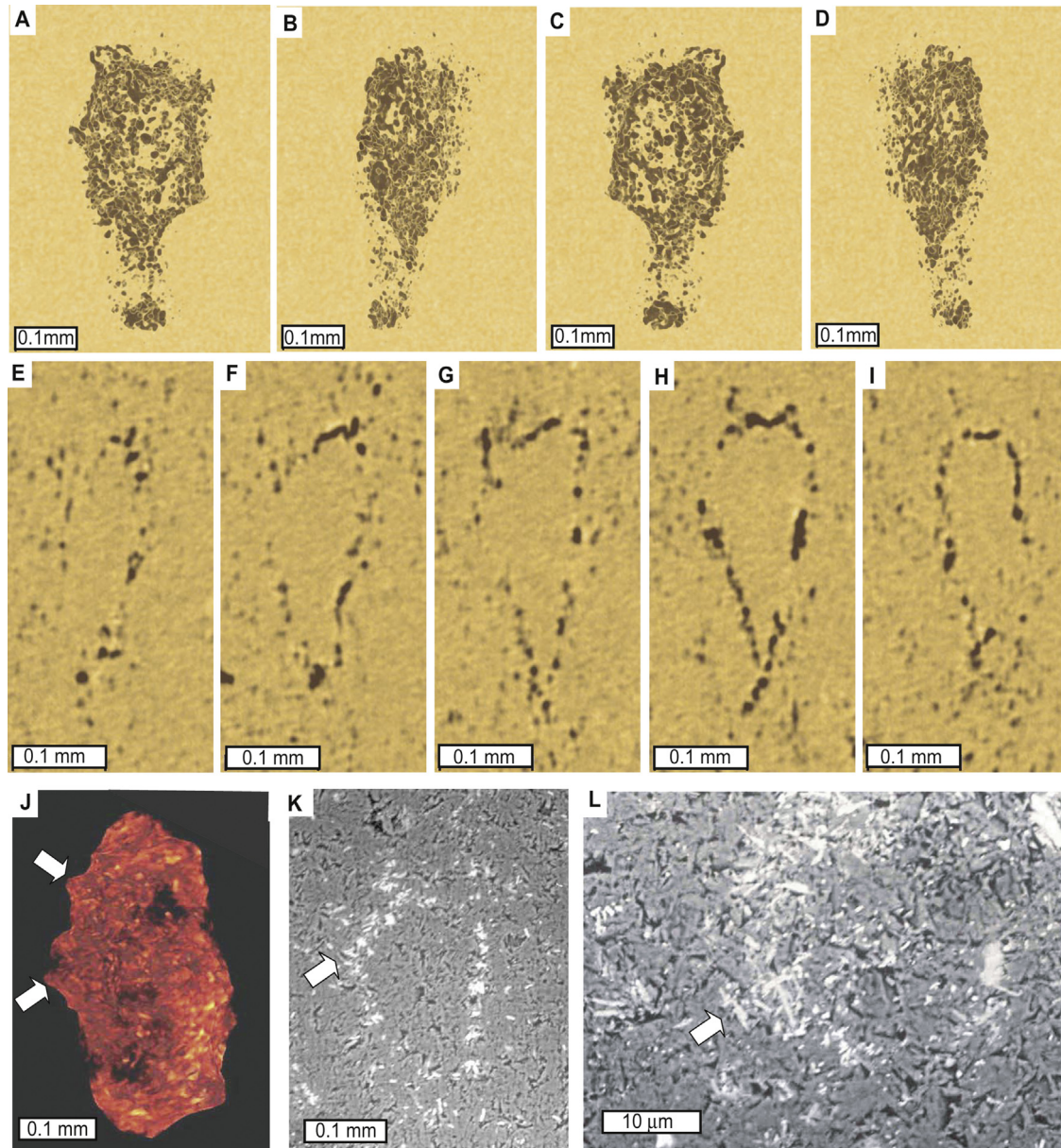


Fig. 5. Three-dimensional rendering (A–D, J), serial sections (E–I) and scanning electron micrographs (K–L) of *Diskagma buttonii* Retallack gen. et sp. nov. Arrows in panels J–L are hollow spines. Three-dimensional renderings (A–D, J) were made (by Parkinson) using Aviso 6.2 software (vsg3d.com) from X-ray synchrotron microtomographic serial sections (E–I) from beamline 8.3.2 at Lawrence Berkeley National Laboratory, and are available also as a rotating video in Supplementary Inline Material. Scanning electron micrographs were obtained from an ISI SS-40 scanning electron microscope.

Modified from Retallack and Krinsley (1993).

The Hekpoort Formation of the Transvaal Basin, and laterally equivalent Tsatsu Formation of Botswana and Ongeluk Formation of the Griqualand West Basin (Fig. 1) includes flood basalts covering at least 200,000 km² of the Kaapvaal Craton of South Africa (Oberholzer and Eriksson, 2000; Ernst and Buchan, 2002; Mapeo et al., 2006). Hekpoort basaltic andesite has been dated by whole rock Rb/Sr at 2184 ± 76 Ma, and the laterally equivalent Ongeluk Formation lavas more accurately at 2222 ± 12 Ma by U–Pb isochron (Cornell et al., 1996). The Bank Break pedotype at Daspoort Tunnel (Fig. 1: underlying the Waterval Onder paleosol) has a Rb/Sr metamorphic age of 1925 ± 32 Ma (Macfarlane and Holland, 1991), perhaps related to intrusion of the Bushveld Complex, which includes the Rooiberg felsite dated by U/Pb at 2061 ± 2 Ma (Walraven, 1997), xenoliths with retrograde metamorphic titanite dated by U–Pb at 2058.9 ± 0.8 Ma (Buick et al., 2001), and Dullstroom Basalt dated by Rb/Sr whole rock at 2071

($+94/-65$) Ma (Buchanan et al., 2004). Another bracketing Re–Os age on early diagenetic pyrite is 2316 ± 7 Ma for the Timeball Hill and Rooihogte Formations (Hannah et al., 2004). Given the stratigraphic position of the Hekpoort Formation within the Pretoria Group (Table 1), an age of 2.2 Ga is corroborated by these bracketing ages.

3.2. Plausible environment for life

The problematic structures are within the surface of a paleosol, first recognized by Button (1979). This paleosol has been called the “Hekpoort paleosol” (thus inviting confusion with the formation name), and regarded as a single, thick, deeply weathered lateritic paleosol, but severely eroded at Waterval Onder (Button and Tyler, 1981; Beukes et al., 2002; Yamaguchi et al., 2007). The Waterval Onder exposure however has characteristic

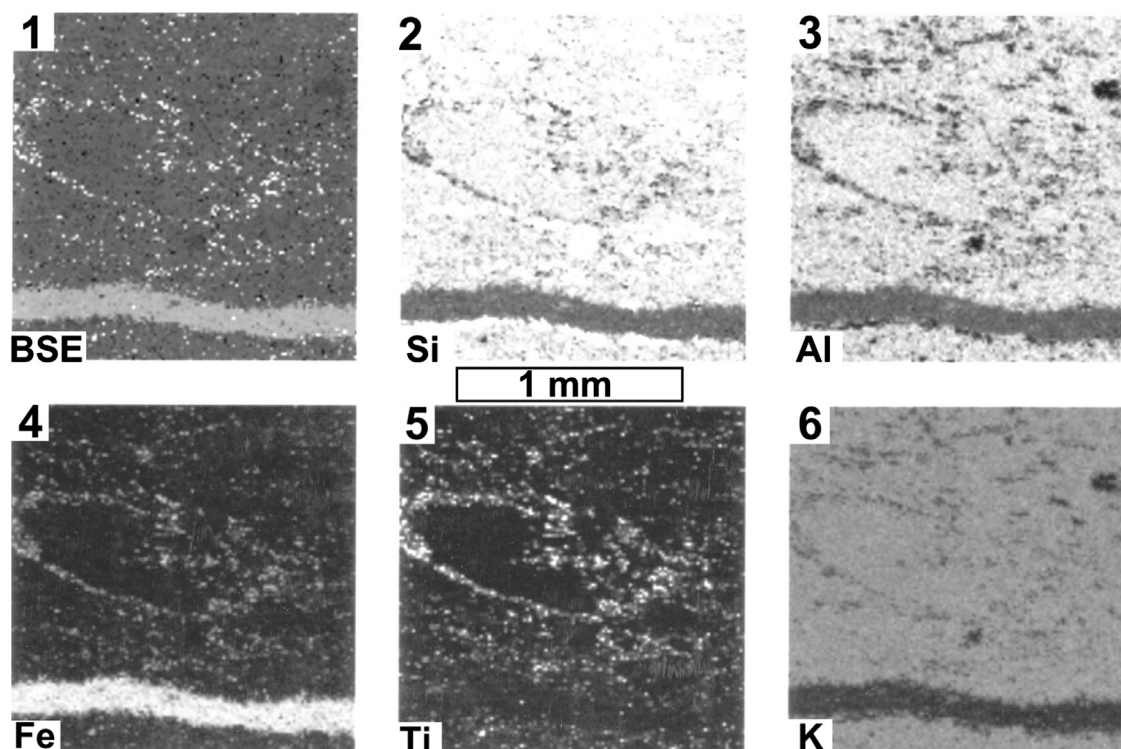


Fig. 6. Back scatter images and element maps (light color is positive for element) of a single example of *Diskagma buttonii* Retallack gen et sp. nov. using a Cameca X50 iron microprobe (by Krull).

surface deformation of a Vertisol paleosol (Fig. 1), and cannot have been an eroded or deeply weathering horizon of a lateritic profile (Retallack, 1986, 2010), nor a hydrometamorphically altered shear zone (Palmer et al., 1989; Retallack, 1989). Another misconception about the Waterval Onder paleosol is that it developed from Hekpoort Formation basaltic andesite, as argued from resistate element ratios by Holland (1984) and Rye and Holland (2000a,b). However, Maynard (1992) and Driese (2004) found resistate element (Ti, Zr and Al) ratios varied beyond acceptable limits (>50% for Ti/Al and >40% for Ti/Zr) for a single parent material (as shown here in Fig. 2), and supported the reconstruction of Retallack (1986) that the profile developed on tuffaceous alluvium overlying the andesite (Fig. 3). The profile studied here is best called the Waterval Onder paleosol (Retallack, 1986), and was one of a number of other pedotypes found on this complex ancient landscape at the top of the Ongeluk-Hekpoort Volcanics. Paleocurrents and thickness variation of the Dwaalheuvel Formation (Button, 1975) are evidence of a hilly terrane with general southwesterly paleoslope from ancient highlands of the Barberton Mountainland to the east. Paleosols formed directly on Hekpoort Formation andesites were too oxidized by modern weathering for detailed geochemical study near Waterval Onder (Fig. 2), but can be called the Bank Break pedotype (perhaps a Viridisol *sensu* Retallack, 2013a), because known unweathered from boreholes at Bank Break, as well as near Potchefstroom, and below a shale (now sericite) at Daspoort Tunnel (Fig. 1: Rye and Holland, 2000a,b). In addition, the top of the laterally equivalent Ongeluk Formation has two strongly ferruginized pedotypes (Oxisols), the Sishen pedotype (also known near Gaborone and Drakenstein: Wiggering and Beukes, 1990; Beukes et al., 2002; Yamaguchi et al., 2007; Yang and Holland, 2003) and an unconformity at the same stratigraphic level has the Wolhaarkop pedotype developed on Kuruman Banded Iron Formation (Holland and Beukes, 1990).

Evidence that the Waterval Onder paleosol was alive, with microbes at least, comes from petrographic and geochemical

observations. Button (1979) and Retallack (1986) observed that in oriented thin sections the upper surface of clayey clasts, and some of the problematic structures as well, were more heavily encrusted in opaque oxides than lower surfaces (Fig. 2B). This arrangement is similar to rock varnish, a common birnessite (non-crystalline iron–manganese) encrustation of desert and other soils (Dorn and Oberlander, 1982), known to be produced by a variety of microbes, especially iron and manganese fixing bacteria, but also other bacteria, algae, and fungi (Staley et al., 1982; Nagy et al., 1991). In support of this idea, both Fe^{2+} and Fe^{3+} increase dramatically in these upper cumulic horizons of the paleosol (Fig. 2).

Another line of evidence for life in this paleosol is the marked near-surface strain-corrected molar depletion of phosphorus and copper in the paleosol, but enrichment in the cumulic surficial swales (Fig. 3). Experimental studies of weathering by Neaman et al. (2005) have shown that such depletion of phosphorus is not possible from abiotic weathering and requires organic ligands, such as acetate and oxalate. Similar phosphorus depletions are produced by a wide array of life, including cyanobacteria, fungi, lichens and land plants. An important caveat of Neaman et al. (2005) is the relative abundance of apatite, which has not been detected by point counting nor X-ray diffraction of the upper part of the Waterval Onder paleosol (Button, 1979; Retallack, 1986). Copper depletion (also noted for the Waterval Onder paleosol in Fig. 3) was found in the weathering experiments of Neaman et al. (2005) to be related to aromatic ligands, such as gallate and salicylate, unique to eukaryotic organisms, such as fungi, lichens and land plants. Potentially cupriferous pyrites in the surface of the Waterval Onder paleosol are 1–2 mm cubic crystals with high positive sulphur isotopic ratios ($\delta^{34}\text{S}$ +6.6, +7.2 and +9.9‰ versus Canyon Diablo troilite) of late diagenetic sulphides (Retallack and Krinsley, 1993).

Highly seasonal climate, with a protracted dry season is characteristic of Vertisols, and can be inferred from the mukkarra structure of the paleosol (Retallack, 1986; Driese, 2004). The degree of

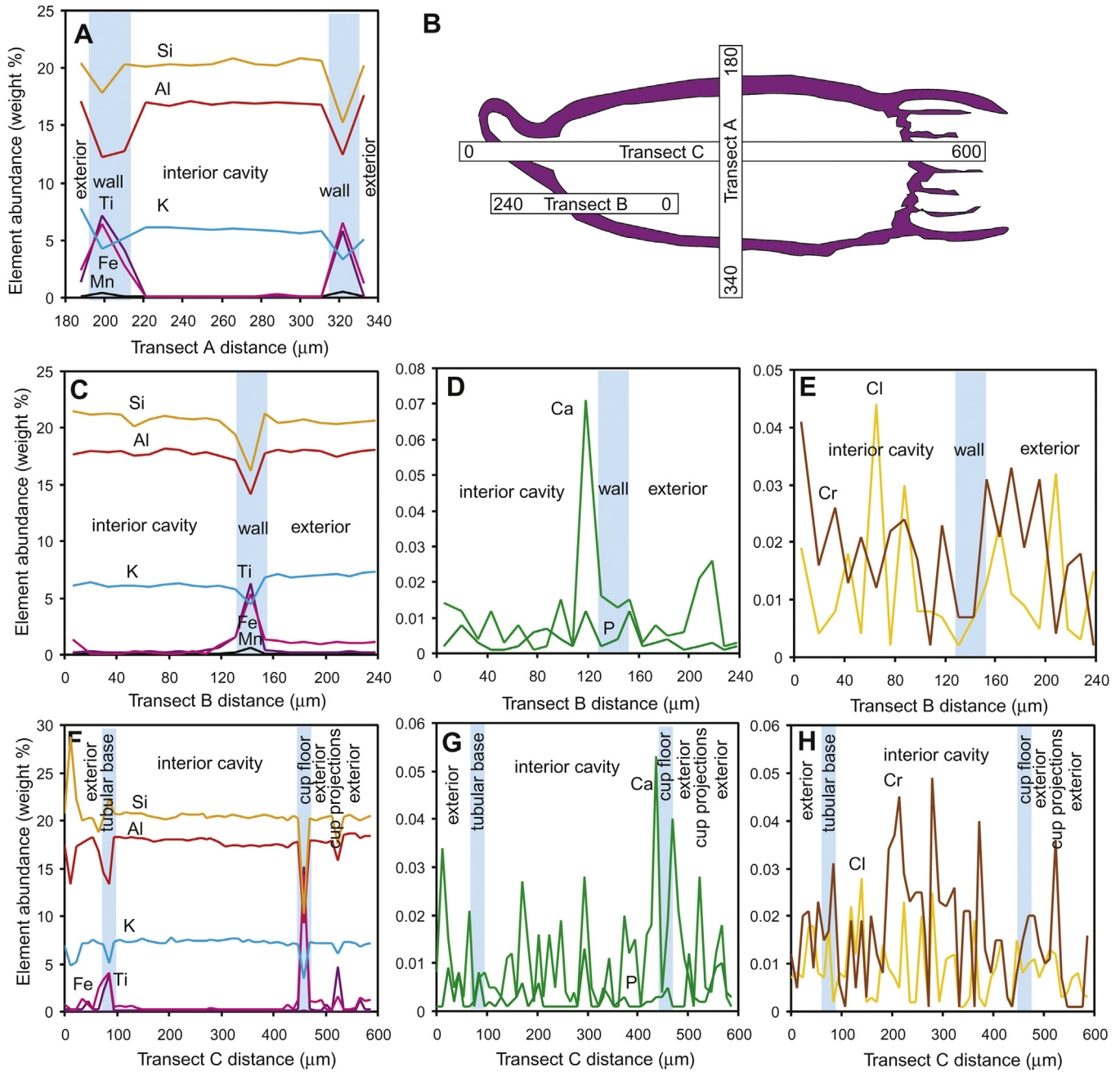


Fig. 7. Element analyses of transects of varied orientation (B) of a single example of *Diskagma buttonii* Retallack gen et sp. nov. using a Cameca X50 iron microprobe (by Krull).

weathering, reconstructed clay mineralogy and lack of carbonate in the Waterval Onder paleosol were used as evidence for a subhumid to humid and warm to cool temperate paleoclimate by Retallack (1986). This can now be refined to a cool temperate humid climate (mean annual temperature $11.3 \pm 4.4^\circ\text{C}$, and mean annual precipitation $1489 \pm 182\text{ mm}$), using subsequently published paleoclimatic proxies (equations 3 and 4 here after Sheldon et al., 2002) for modern soils applied to the chemical composition of the uppermost yellow sericite sample (50 cm in Fig. 3). This paleoclimate is intermediate between that inferred for Makganyene Glaciation of the Griqualand West Basin at a stratigraphic level of the basal Rooihogte Formation (Kopp et al., 2005; Bekker et al., 2005), and tropical perhumid weathering inferred from the Sishen and Wollaarkop paleosols at stratigraphic levels equivalent to the Dwaalheuvelformation (Beukes et al., 2002; Yamaguchi et al., 2007).

Atmospheric CO_2 levels can affect habitability of soils, because mass extinctions coincide with spikes of high CO_2 , such as $7832 \pm 1676\text{ ppm}$ determined from seed fern stomatal index during the Late Permian life crisis (Retallack, 2013b). An estimate for atmospheric CO_2 of 6640 (+12880/–4293) from the Bank Break paleosol (underlying the Waterval Onder paleosol), used base depletion, paleoclimate and soil duration estimates (Sheldon, 2006). This result is compromised by evidence for life in the paleosols presented here (molar phosphorus depletion of Fig. 3), which could account for as much as half the CO_2 estimate in the climatic regime envisaged for the Waterval Onder paleosol (Retallack, 2009). This exacerbates the problem that Sheldon's (2006) estimate is insufficient to overcome the faint young sun at 2.2 Ga in creating soils that lack periglacial features (Kasting and Catling, 2003). Additional greenhouse gases such as $\text{H}_2\text{--N}_2$ interaction and CH_4 are needed

because atmospheric pressure by 2.7 Ga was comparable with modern (Som et al., 2012; Wordsworth and Pierrehumbert, 2013).

The Waterval Onder paleosol also has been used to calculate O_2 levels (Holland, 1984), which is important for the habitability of soils because oxygenation of at least 1–2% is needed develop a full UV shield of stratospheric ozone (Kasting and Catling, 2003). A low atmospheric O_2 estimate of 0.08% from the Waterval Onder paleosol (Holland, 1984; Rye and Holland, 2000a,b) is no longer valid because key assumptions are incorrect: the Waterval Onder paleosol did not form on basalt and was not biologically sterile (Maynard, 1992; Driese, 2004; Retallack, 1986; Retallack and Krinsley, 1993; Ohmoto, 1996; Holland et al., 1997). Broad limits of 0.1–1% atmospheric O_2 were derived from Retallack's (1986) geochemical study of the Waterval Onder paleosol assuming originally sedimentary parent material at 210 cm and wide limits of CO_2 (Fig. 3). Another way of looking at the problem has been provided by Neaman et al. (2005) whose laboratory studies of weathering showed that depletion of Cu (as seen in Fig. 3) occurs in oxidized (ambient modern), but not anoxic ($O_2 < 10^{-6}$ atm), biologically active soils. The 2.2 Ga Waterval Onder paleosol is younger than the Great Oxidation Event dated at 2.45 Ma from decline of mass independent fractionation of sulfur in evaporates (Farquhar and Wing, 2003) and 2.33 Ma from onset of positive organic carbon isotopic excursions and red beds (Bekker and Holland, 2012). Estimates for 2.2–2.1 Ga of 0.9–5% atmospheric O_2 come from a Sishen pedotype paleosol at Drakenstein and the Wolhaarkop paleosol (Bekker and Holland, 2012) and of 0.1–1.0% atmospheric O_2 from cool-climate extremes of an array of Paleoproterozoic paleosols (Murakami et al., 2011). These estimates are compatible with what is now known about the Waterval Onder paleosol, which thus formed in a mildly oxidizing atmosphere with an effective ozone shield from UV radiation, but at least an order of magnitude less oxygen than the modern atmosphere (21% O_2). The problematic structures described here were thus from rocks of a plausible surface environment for life, with benign climate and moderate ultraviolet radiation.

3.3. Same age as the rock

The problematic structures were not endolithic organisms introduced in outcrop within the deep road cut (Fig. 2A), long after burial of the Waterval Onder paleosol, because they have been profoundly altered by greenschist facies metamorphism associated with intrusion of the 2.0 Ga Bushveld Complex (Retallack and Krinsley, 1993). The putative fossils are truncated and disrupted in thin section by veins of berthierine (Fig. 4D) due to greenschist facies metamorphism, because of their included chloritoid and stilpnomelane (Retallack, 1986). These veins are straight-sided and have little opaque oxide, unlike stylolites (Andrews and Railsback, 1997). In addition, the walls of the putative fossils examined at high magnification by back-scatter electron microscopy are completely recrystallized to iron silicates of the same grain size and texture as the rest of the sericitic matrix (Fig. 5K and L). This line of evidence constrains the age of the problematic structures to greater than 2.0 Ga regional metamorphism by the Bushveld Complex.

Observations of density and attitude of the structures make it unlikely that the problematic structures were introduced into the paleosol after covering by the Dwaalheuveld Formation (ca. 2.2 Ga) and before metamorphism (ca. 2.0 Ga). The structures locally comprise most of the volume of the rock. Individual bedding planes of the cumulic A horizon of gilgai swales of the paleosol observed in thin section contain a standing density of $276,607 \pm 22,854$ (mean and standard deviation) individuals per m^2 of former soil surfaces. The problematic structures are clumped within particular layers of the surface gilgai swale (Fig. 2), and were not found deeper within the profile. They are arrayed at

various orientations, generally concordant with crude laminations of this part of the profile. They attach to narrow tubular structures which zig-zag along and down into the rock (Fig. 4K and L). Some are near vertical or obliquely stacked, and if in a group they radiate outward (Fig. 4A). These orientations are compatible with a model in which they were attached to the substrate and originally erect, but fell over as surface increments of sediment were deposited within the seasonal ponds (gilgais) of the Vertisol. They are not imbricated, graded or sorted like alluvial clasts illustrated by Rhodes et al. (2005), nor strata-transgressive like endolithic organisms illustrated by de la Rosa et al. (2012).

3.4. Plausible biotic composition

Genuine fossils must also demonstrate plausible organic, organomineral or taphonomically altered biogenic composition. Total organic carbon of the samples was 0.04% and the isotopic composition of organic carbon ($\delta^{13}C$) was $-25.6 \pm 0.08\%$ (two standard deviations) versus Vienna Pee Dee Belemnite standard. This is a common isotopic value for photosynthetic organisms, particularly cyanobacteria, other photosynthetic bacteria, eukaryotic algae, lichens, vascular land plants, liverworts, hornworts and mosses (Schidlowski et al., 1983; Jahren et al., 2003; Fletcher et al., 2004; Tomescu et al., 2009), as well as for saprophytic fungi using such plants as substrates (Hobbie and Boyce, 2010).

Organic matter can be seen as dark material (low atomic number) in back-scatter scanning electron micrographs. These dark areas are about 7% by volume of the walls of the structures (Fig. 5L) and 2% by volume of matrix (Fig. 5K). Dark carbon is within the interstices of berthierine and iron–manganese–titanium oxide grains (gray to white and high atomic number in Fig. 5K and L) recrystallized by metamorphism to 300–400 °C, 2–4 kbar pressure and 10–16 km depth of burial (Retallack and Krinsley, 1993). This amount of metamorphism is typical for Appalachian Paleozoic fossils analyzed for carbon isotopic composition, and for carbon isotopic analyses of Precambrian rocks found to have unenriched values comparable with modern plants (Schidlowski et al., 1983; Tomescu et al., 2009). Significant enrichment of carbon isotopic composition (high $\delta^{13}C$) is found in organic matter subjected to amphibolite facies metamorphism, like the Isua supracrustals of Greenland (Schidlowski et al., 1983). Microprobe element mapping reveals that the yellow matrix inside the structures and also outside them is a K–Al–silicate mineral (Fig. 6). The walls themselves are not only enriched in organic carbon, but also in Fe and Ti, with lesser amounts of Mn and P (Fig. 7).

Just as the sericite (K–Al–silicate) is a likely recrystallization product of illite and kaolinite (Retallack, 1986; Retallack and Krinsley, 1993), the white crystals in back-scatter images (Fig. 5K and L) may be recrystallized from colloidal precursor material, probably a birnessite (Fe–Mn colloid) encrustation and impregnation of an original organic wall. Such colloidal coatings (mangans) are common in modern soils (Rahmatullah et al., 1990) and paleosols (Retallack et al., 2000).

The problematic structures of the Waterval Onder paleosol may have been encrusted with biofilms from bacterial decay of organic matter, as is common in rock varnish (Staley et al., 1982; Nagy et al., 1991). Predepositional death masks of ferric hydroxide on an organic matrix are an explanation for fine preservation of fossil leaves such as those of the Cretaceous Dakota Formation of Kansas (Retallack and Dilcher, 2012), based on observations of rusty coatings of modern leaves created by *Sphaerotilus natans* (Spicer, 1977). These filamentous proteobacteria settle on surfaces by entanglement and by an adhesive base (Pellegriin et al., 1999).

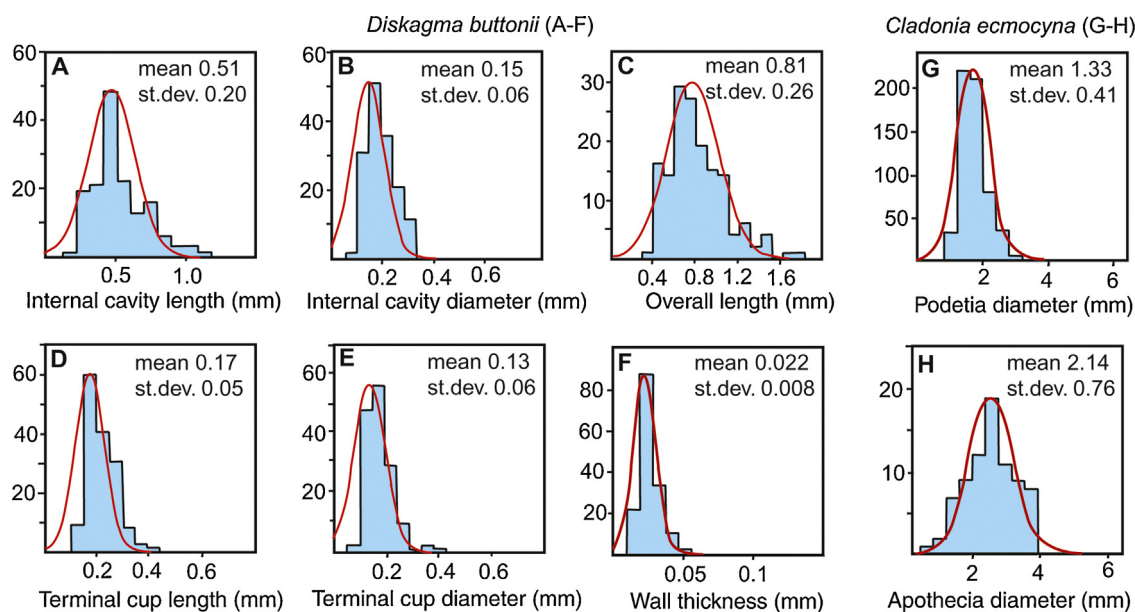


Fig. 8. Size distribution of *Diskagma buttonii* Retallack gen. et sp. nov. and the living lichen *Cladonia ecmocyna* (by Retallack). Curves are contrasting computed normal distributions with the same mean and standard deviation: most of these distributions are negatively skewed as expected of indeterminate growth.

Sphaerotilus, and the similar *Leptothrix* are heterotrophic, and their accumulation of iron hydroxides and oxides is fueled by decay of organic matter. Although widely considered iron-oxidizing bacteria, iron does not seem necessary for metabolism of *Sphaerotilus* and *Leptothrix*, but iron oxidation is catalyzed by their particular bacterial exopolysaccharides (van Veen et al., 1978).

Another alternative is that the problematic structures were bioaccumulator organisms, preferentially taking up metals such as Fe, Mn, Ti, Cu and Cr (Figs. 2 and 7) as well as Ni (Retallack, 1986), like modern lichens (Sawidis et al., 1995), mosses (Basile et al., 2008), earthworms (Suthar et al., 2008), aquatic invertebrates (Rainbow, 2006) and fish (Luoma and Rainbow, 2006). This explanation is not appealing for the Waterval Onder metal accumulations which are now recrystallized berthierine or opaque oxides, because bioaccumulated metals are retained in reduced and chelated form.

Biological encrustation and bioaccumulation are common reasons for preservation of fossils in paleosols (Retallack, 2011; Retallack and Dilcher, 2012), but most biologically active soils and paleosols are organic-lean (Retallack, 1991). Exceptions are the peaty surface horizons of Histosols and cumulic horizons of Vertisols swales, where fossils may be preserved by successive increments of flood accumulation (Driese et al., 1992; Retallack, 1997). Similarly in the Waterval Onder paleosol, putative fossils are locally abundant in strata-concordant dark layers of swale fill, but not seen in the yellow soil matrix (Fig. 2)

3.5. Taphonomic series

Organisms are recyclable, and their fossils betray signs of varied decay, boring or comminution, in all but the best preserved specimens. The Waterval Onder structures can be arranged in series of varied distinctness and thickness of walls, deflation of the central cavity, and decay of the extremities, while maintaining debris-free interiors (Fig. 4D–J). These observations rule out interpretation of these structures as ellipsoidal volcanic vugs (Cashman and Kauahikaua, 1997), pedogenic vesicles (McFadden et al., 1998), gas escape structures (Frey et al., 2009), sedimentary clasts (Button, 1979), pedogenic nodules or crumb peds (Retallack, 1986). Distinct mineral fills of agates, carbonates or zeolites are found in vesicles and other hollow cavities degraded by soil formation, whereas solid

objects in soils are corroded and embayed by weathering (Delvigne, 1998). Pedogenic and sedimentary nodules in addition often show fused forms and relict internal bedding and grains (Potter et al., 2011), not seen in the Waterval Onder structures. Nodules also have distinct chemical composition, such as calcite, siderite or hematite (Kauffman and Steidtmann, 1981; Potter et al., 2011). In contrast, our Cameca SX50 microprobe mapping of the Waterval Onder structures (Figs. 6 and 7) demonstrates that their fill is sericite, chemically and texturally similar to their matrix.

Organisms also show growth series and a predictable size range. The Waterval Onder paleosol structures show unimodal size distributions with low standard deviation (Fig. 8). They are log-normal (Inline Supplementary Material Table S2) as in perennial organisms with indeterminate growth, such as lichens, plants and colonial corals or bryozoans (Retallack, 2007, 2011). In contrast, nodules, crystallaria and Martian “blueberries” show high-variance, poly-modal size distributions (Kauffman and Steidtmann, 1981; Potter et al., 2011), and most microbes, protists and animals show Gaussian normal distributions of organisms with determinate growth (Schopf et al., 2010).

Growth of the problematic structures was orthometric (Fig. 9) rather than allometric, maintaining constant proportions of the central hollow and terminal cup. The nearly circular cross sections of the structures were measured across and within bedding within oriented thin sections not as an indication of growth, but as an indication of burial compaction (Fig. 9D) under about 10 km of overlying Pretoria Group and Bushveld Complex (Kent, 1980). The inferred burial compaction fraction of 0.53 can be added to the slopes of the other orthometric relationships (Fig. 9A–C) to approximate the growth proportions of uncompacted structures.

Differences between observed compaction of the structures and that of the host paleosol offer additional insights into potential biopolymers of the problematic structures. Ptygmatic deformation of clastic dikes in the Waterval Onder paleosol is evidence that it was compacted to 67–73% of its former thickness (Retallack, 1986) as expected for Vertisols buried so deeply (following equation 5 after Sheldon and Retallack, 2001). Measurements of vertical to horizontal diameters of the most nearly circular examples of the problematic structures and their tubular bases (Fig. 9D) show compaction to 53% of their former thickness, indicating that their

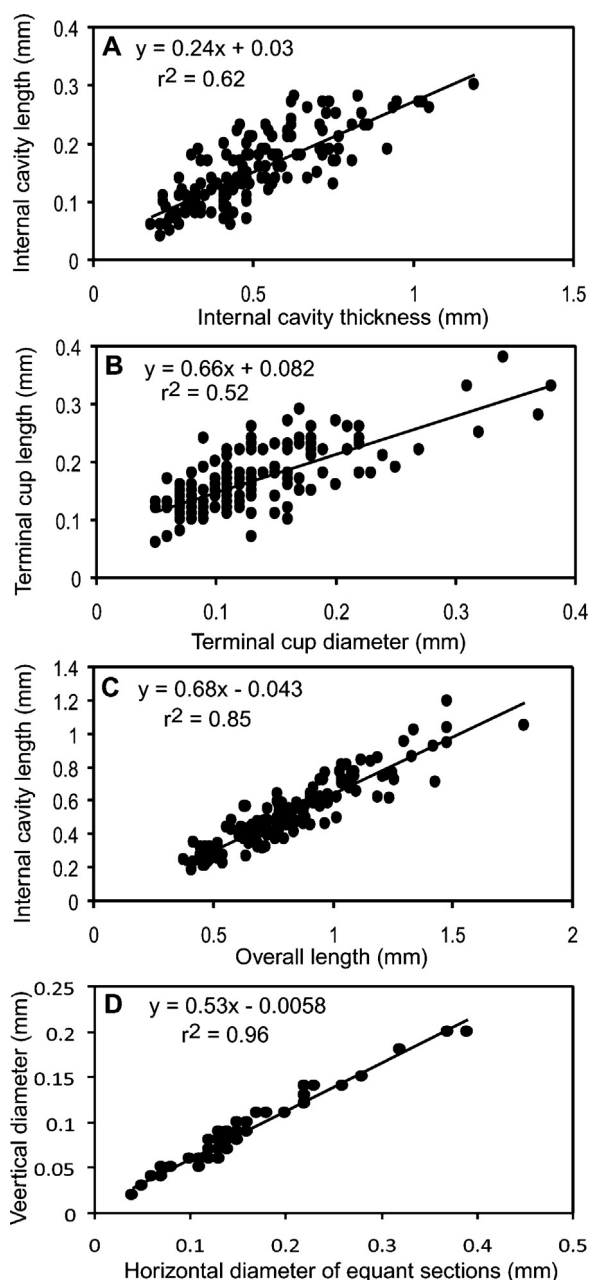


Fig. 9. Correlated measurements of *Diskagma buttonii* Retallack gen et sp. nov. in thin sections (by Retallack).

compaction followed a compaction curve established for fossil fungi (Eq. (6)) rather than a curve established for burial compaction of fossil logs (Eq. (7)). This unusual compaction resistance of the fossils (Fig. 10) is evidence for some kind of biopolymer such as chitin in the walls enabling the structures to resist crushing before reinforcement by metamorphic recrystallization. Like Ediacaran fossils, *Prototaxites*, *Spongiophyton* and *Thucomyces* (Retallack, 2007), these Waterval Onder structures were more compaction-resistant than wood. This conclusion relies on the assumption that the structures were empty during the critical first kilometer of burial, when most fossil compaction occurs (Fig. 10), and that the limpid fill of the structures is an early diagenetic cement like the intergranular cement of the Dwaalheuveld Formation. If the hollow structures were torn and filled with clay before burial, then their greater compaction compared with their enclosing paleosol would reflect partial fill, rather than strong biopolymer walls. It would be

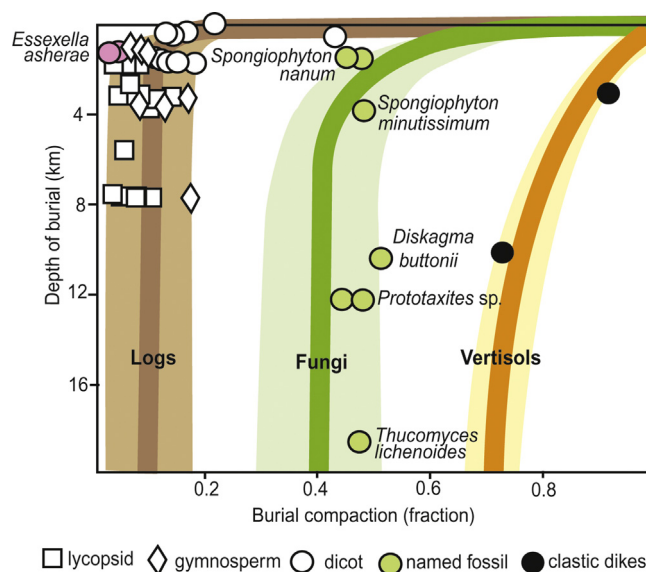


Fig. 10. Compaction of *Diskagma buttonii* Retallack gen et sp. nov and other fossils compared with the Waterval Onder clay paleosol and a variety of fossil logs and jellyfish.

Modified from Retallack (2007).

partial fill, because the structures are not as compaction resistant as the matrix (Fig. 10). If there were partial fill, however, some of the opaque grains so common outside the structures should have found their way into them.

3.6. Repeated complexity

Abundant problematic structures within the surface of the Waterval Onder paleosol are unlikely to have been pseudofossils because of their structural complexity: urn-shaped with a large central hollow, leading to hollow tubular base, and at the other end, a cup-shaped structure containing poorly preserved parallel filaments (Fig. 4). The torn and branching filamentous remnants within the cup-shaped end are particularly complex and intriguing: sadly their details are obscured by micrometer scale recrystallization (Fig. 5K). Hollow spine-like protuberances atop broader mounds, especially evident from microtomographic imaging (Fig. 5A–D and J), are also distinctive complexities. The fossils are not deformed spheroids, but elongate structures, as proven by synchrotron X-ray tomography (Fig. 5A–I). Furthermore, this flared-urn shape is repeated in hundreds of specimens examined in thin section in which the various measurable elements remain in fixed proportions (Fig. 9).

The degree of complexity of these structures is well short of that seen in trilobites or brachiopods, but comparable with that of other Precambrian fossils such as the 1.9 Ga spiral compression *Grypania spiralis* (Han and Runnegar, 1992; Schneider et al., 2002), the 1.5–1.1 Ga string of beads *Horodyskia williamsi* (Grey et al., 2010; Retallack et al., 2013), 0.55 Ga bead-like *Funisia dorothea* (Droser and Gehling, 2008), the 0.55 Ga flanged pit-and-mound of *Coronacollina acula* (Clites et al., 2012), and the 0.55 Ga goblet-shaped *Namacalathus hermanastes* (Grotzinger et al., 2000).

4. Systematic paleontology (by G.J. Retallack)

For reasons outlined in the preceding sections, the enigmatic structures of the Waterval Onder paleosol are regarded as biogenic, and are here designated *Diskagma buttonii* Retallack gen. et sp. nov. A possible life restoration decompacted (Figs. 9D, 10) from X-ray microtomographic images (Fig. 5A–D) is given in Fig. 11.

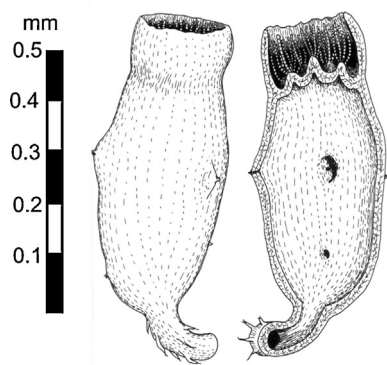


Fig. 11. Interpretive reconstruction of the holotype specimen of *Diskagma buttonii* exterior (left) and in cross section (right).

Biological affinities of fossils from the Waterval Onder paleosol remain uncertain, and the new taxon proposed here is best suited to liberal provisions of form genera within the International Botanical Code (McNeill et al., 2006).

4.1. Genus

Diskagma Retallack gen. nov.

4.2. Type species

Diskagma buttonii Retallack gen. et sp. nov.

4.3. Diagnosis

Elongate, urn-shaped, hollow structures, attached in groups to a basal hollow tubular structure; urn-shaped body has hollow spines on broad protuberances, and basal hollow tubular structure has radiating solid filamentous branching structures; organic walls thin and opaque, encrusted with iron and manganese oxides; a terminal cup has an irregular floor and poorly preserved branching filamentous structures running more or less parallel toward the opening.

4.4. Etymology

The new genus and epithet is Greek (δίσκος male, ἄγμα neuter) for “disk-like fragment”, paraphrasing Button’s (1979) brief description of these features.

4.5. Species

Diskagma buttonii Retallack sp. nov. (Fig. 4A and G).

4.6. Diagnosis

Diskagma with short (0.3–1.8 mm) and narrow (0.1–0.3 mm) hollow structures, arranged in groups of 3–4 around the basal tubular structure.

4.7. Description

These small fossils do not show up well in spilt slabs, because they are of comparable color to their matrix (Fig. 4K–P). They are best seen in petrographic thin sections, in which their inclusion-free sericitic fill is eye-catching (Fig. 4A–J). The overall structure as reconstructed from X-ray tomography is like an urn with flaring lip above an irregular, subhorizontal wall (Fig. 5A–I). The base of the structure tapers to a narrow, hollow tube, which zigzags

through matrix connecting several individuals and solid tapering and branching filamentous structures (Fig. 4K–L).

A few (3–4 per hollow structure), widely scattered, large hollow protrusions of the wall deform the curved urn shape in X-ray tomographic reconstruction (Fig. 5A–D). These culminate in truncated hollow tubes directed outwards (Fig. 5E–I). Such features are not common enough to disrupt the curved biconvex profile of the inner cavity in most thin sections (Fig. 4D–J). The naturally fractured specimens show such protrusions, as well as a vertically striated appearance from subvertically aligned filamentous structures (Fig. 4M–P).

Opaque filamentous structures within the terminal cup are poorly preserved because of metamorphic crystallization at the micron scale (Fig. 4C). These filamentous structures are vertical to the irregular floor of the cup and form a subparallel, branching array connected to mounds of the cup floor. Some of these structures have the appearance of chains of cells, but may be displacive crystals of berthierine (Fig. 4B and C).

4.8. Occurrence and range

Swale in surface horizon of Waterval Onder palaeosol, in road-cut 2.7 km west of Waterval Onder, Transvaal, South Africa (S25.645330° E30.357676°): upper Hekpoort Formation (2.2 Ga), Pretoria Group of Transvaal Basin.

4.9. Etymology

This species is named in honor of Dr A. Button.

4.10. Holotype

Condon Collection, Museum of Natural and Cultural History, University of Oregon thin section F116533A. Paratype specimens in the same collection include F116530–F116534 inclusive.

5. Comparable fossils

An Archean fossil of comparable morphology and size to *Diskagma* is *Thucomyces lichenoides* (Fig. 12F–G) dated to 2.8 Ga (Schaefer et al., 2010) from the Carbon Leader of the Central Rand Group near Carletonville, South Africa (Hallbauer and van Warmelo, 1974; Hallbauer et al., 1977; Mossman et al., 2008). Like *Diskagma*, *Thucomyces* tubes are 2–3 mm long by 0.5–0.6 mm in diameter, and form dense palisades on the surface of paleosols (Mossman et al., 2008). Unlike *Diskagma*, *Thucomyces* is filled with complex vertical partitions, lacks scattered spine-like extensions, and has mostly rounded terminations. Some ends of *Thucomyces* are indented and flanged, but more like a turban than a cup (Fig. 12F). Also unlike *Diskagma*, *Thucomyces* has very light isotopic compositions averaging -28.1% (mostly ranging from 27.1 to -32.8% , but including two outliers of -22.4 to -22.9% : Hoefs and Schidlowski, 1967). Organic matter of *Thucomyces* also has pentose/hexose ratios of 1, and chlorophyll-bacteriochlorophyll derivatives such as pristane and phytane (Prashnowsky and Schidlowski, 1967). The trace elements bioaccumulated by, or biofilmed onto, *Thucomyces* are also different, including native gold and uranium (MacRae, 1999; Mossman et al., 2008). *Thucomyces* was regarded by Cloud (1976) as an artifact of bubbling action of HF acid used to extract them from the matrix, and by Barnicoat et al. (1997) as blebs of mobilized postmetamorphic hydrocarbon, but these interpretations are falsified by observations of *Thucomyces* palisades cut by metamorphic veins (MacRae, 1999) and redeposited within sediments of the same stratigraphic horizons (Mossman et al., 2008). Oxygen and hydrogen isotopic composition of the carbon of *Thucomyces*

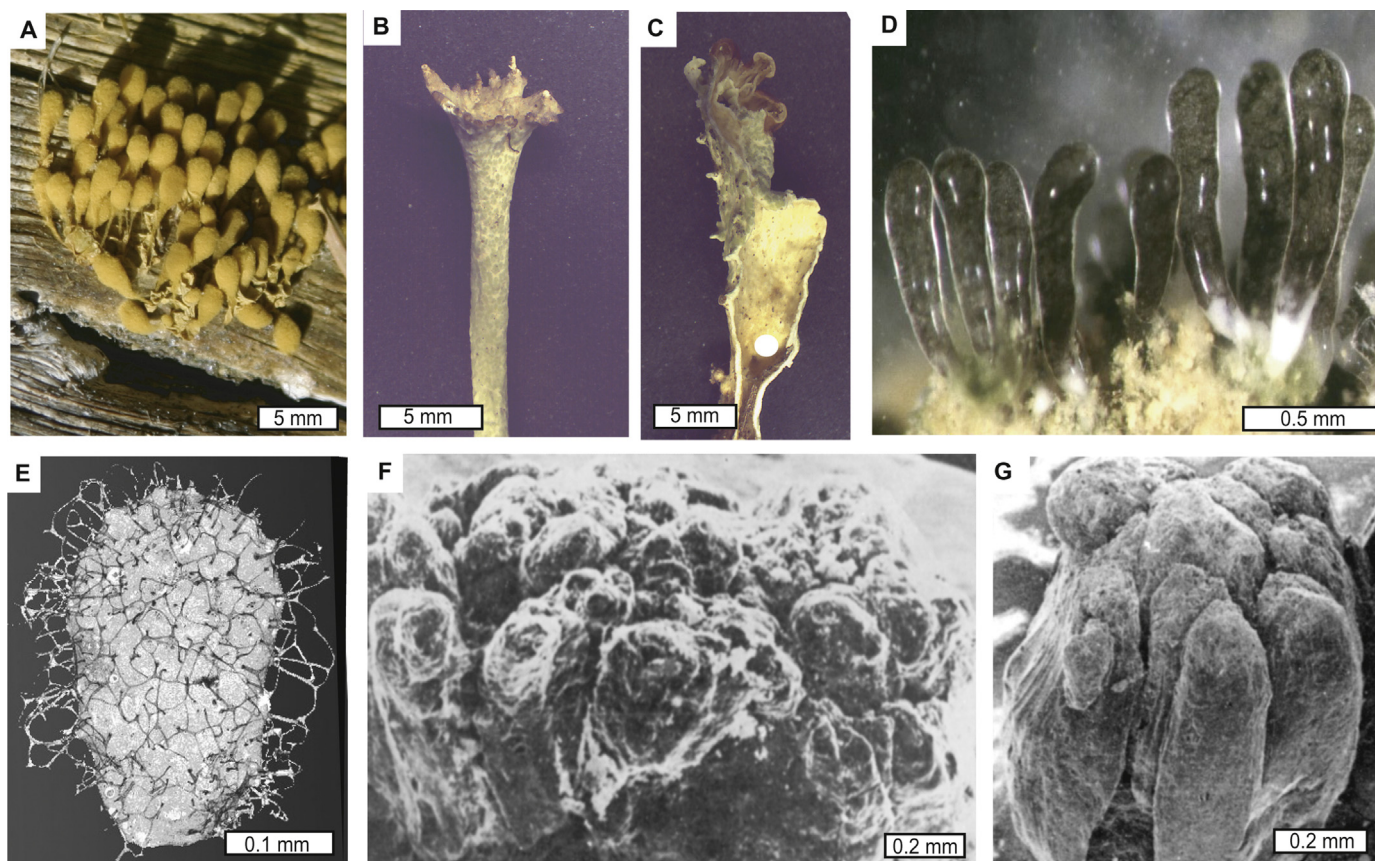


Fig. 12. Living (A–D) and fossil (E–G) organisms comparable with *Diskagma buttonii* Retallack gen et sp. nov.: A, *Leocarpus fragilis* (Physaraceae, Mycetoza) on deadfall of mountain hemlock (*Tsuga mertensiana*) along trail between Hand and Scott Lake, Three Sisters Wilderness, Oregon; B and C, terminal cup and section of hollow *Cladonia ecmocyna* (Cladoniaceae, Ascomycota) from litter 300 m east of outlet of Fishtrap Lake, Montana; D, *Geosiphon pyriformis* (Archaeosporaceae, Glomeromycota) from forest floor near Darmstadt, Germany; E, *Tappania* sp. cf. *T. plana* (problematicum) from ca. 850 Ma Wynnatt Formation, Victoria Island, Nunavut (Butterfield, 2005); F and G, *Thucomyces lichenoides* (Hallbauer and Van Warmelo 1976; Hallbauer et al., 1977) from the 2.8 Ga Carbon Leader, Central Rand Group, Carletonville, South Africa. Images are reprinted courtesy of Arthur Schüßler (D), Nicholas Butterfield (E) and Dieter Hallbauer (F–G).

also rules out metamorphic remobilization (Grové and Harris, 2010).

Another hollow, organic-walled fossil with lateral hollow spine-like protrusions deforming the shape from rounded to polyhedral is *Tappania plana* from the 1.46 Ga Roper River Group of Northern Territory, Australia (Javaux et al., 2001). This fossil is known as a palynomorph much smaller (up to 160 μm) than *Diskagma*. *Tappania* sp. (Fig. 12E) from the 0.82 Ga (Jones et al., 2010), Wynnatt Formation of Nunavut is up to 300 μm long, at the low end of *Diskagma* size range. *Tappania* sp. has spine-like protrusions as well as basal stolon-like attachments (these should be assigned to form genus *Germinosphaera*, as noted by Butterfield, 2005). Both *Tappania plana* and *Tappania* sp. have long branching sparsely septate filaments extending from the spine like protrusions to the wall. It is difficult to rule out such delicate extensions for *Diskagma* because of its coarse metamorphic recrystallization.

Another topologically comparable (hollow elongate fossil with a terminal cup) fossil is *Namacalathus hermanastes* from the 0.55 Ga Zaris Formation of Namibia (Grotzinger et al., 2000). These are larger (2–25 mm diameter of terminal cup) than *Diskagma*, and preserved as calcite casts between thrombolites of pinnacle reefs. Furthermore their terminal cups with lateral openings are much larger than, and connected to, their narrow hollow stalks.

Interpretations of *Thucomyces* and *Tappania* have proven controversial, largely because of the unusual antiquity of these large, complex, and thus putatively eukaryotic fossils. Hallbauer and van Warmelo (1974) and Hallbauer et al. (1977) regarded *Thucomyces* as a lichen, without specifying a particular fungal group.

Mossman et al. (2008) suggested prokaryotic stromatolitic affinities on the basis of filamentous wall structure, but *Thucomyces* lacks domed lamination and mineralization defining stromatolites (Allwood et al., 2006; van Kranendonk et al., 2008). Butterfield (2005) attributed *Tappania* sp. to higher fungi (Basidiomycota-Ascomycota) because of its distinctive fused hyphae, but fused hyphae are also known from Glomeromycota (Bever and Wang, 2005) and Oomycota (no longer regarded as fungi: Berbee and Taylor, 2010a,b). Long, branching, sparsely septate hyphae have also been found attached to 1.5 Ma *Tappania plana* (Javaux et al., 2001), but not fused hyphae. Complexly ornamented large acritarchs like *Tappania* also have been regarded as algal phycmata (Moczydłowska et al., 2011) and metazoan cysts (Cohen et al., 2009). *Namacalathus hermanastes* has been compared with a cnidarian scyphopolyp (Grotzinger et al., 2000, Knoll, 2003), but topologically they are similar to lichen podetia with apothecia, such as *Cladonia* (Fig. 12B and C).

Large size (>100 μm) in itself is not adequate evidence of eukaryotic affinities for organic walled fossils, because prokaryotes such as sulphur bacteria and archaea grow up to 750 μm long (Javaux et al., 2010). Ornament or other indications of a sophisticated eukaryotic cytoskeleton are needed, and are known back some 1.8 Ga among presumed marine acritarchs (Lamb et al., 2009) and 1.2 Ga among lacustrine acritarchs (Strother et al., 2011). Also plausibly, but not conclusively eukaryotic, are large (12 mm) marine-lacustrine fossils: unnamed *Horodyskia*-like fossils from near Franceville (2.1 Ga) in Gabon (El Albani et al., 2010), helical organic compressions of *Grypania spiralis* (1.9 Ga) attributed to siphonous alga (Han and

Runnegar, 1992; Schneider et al., 2002), and connected bead-like impressions of *Horodyskia williamsi* (1.5–1.1 Ma) attributed to glomeromycotan fungi (Grey et al., 2010; Retallack et al., 2013). Terrestrial *Diskagma* at 2.2 Ga and *Thucomyces* at 2.8 Ga are older again, and much older than current molecular clock estimates for eukaryotes at 1.6 Ga (Bhattacharya et al., 2009). Both *Diskagma* and *Thucomyces* have large size (>1 mm) like eukaryotes. Both also are attached to tubular structures like *Horodyskia*, and *Diskagma* has hollow spines like *Tappania*. *Thucomyces* has irregular vertical internal partitions and both floor and roof levels like bacterial biofilms (Hall-Stoodley et al., 2004). *Diskagma* on the other hand is a hollow like the central structures of Franceville fossils (El Albani et al., 2010), *Horodyskia* (Retallack et al., 2013) and *Tappania* (Butterfield, 2005). Unfortunately metamorphic recrystallization has destroyed possible apical sexual reproductive structures in *Diskagma* (Fig. 4B and C) needed to establish its biological identity.

6. Comparable living organisms

Morphologies and sizes of *Thucomyces* and *Diskagma* are unknown in prokaryotes. Actinobacterial sporangia can be comparable in shape but are much smaller (<10 μm) and full of spores (Gnilovskaya, 1985), unlike *Diskagma*. Thalli of the few actinobacterial lichens known (such as *Streptomyces griseus*: Kalakoutskii et al., 1990) are small crustose discs and shallow cups, but not hollow structures like *Diskagma*. Nevertheless, lichen form is so strongly convergent across fungal clades (Brodo et al., 2001), and actinobacterial lichens so poorly known (Kalakoutskii et al., 1990), that this remains a possibility. Other prokaryotic possibilities are bacterial biofilms, which can be columnar, mounded and pustulose (Dunne, 2002; Hall-Stoodley et al., 2004), but are soft, with an array of bubble structures of different sizes, and lack the organization or apparent resistance to burial compaction of *Diskagma*. Columnar bacterial films are plausible for the irregular internal partitions of *Thucomyces*. Columnar bacterial biofilms have both floor and roof platforms, connecting two water levels of planar aquatic biofilms (Hall-Stoodley et al., 2004), more like *Thucomyces* than *Diskagma*. Actinobacteria on land are permitted by molecular clocks as far back as 2.6 Ga (Battistuzzi and Hedges, 2009).

Structures broadly comparable with *Diskagma* in biological soil crusts today include testate amoebae (Porter et al., 2003), sporocarps of slime molds (Fig. 12A), podetia of ascomycotan lichens (Fig. 12B and C), fruiting bodies of fungi (Bon, 1987), and bladders of glomeromycotan endocyanotic lichens (Fig. 12E). *Diskagma* lacked an exoskeleton like testate amoebae (Porter et al., 2003), and internal structures (columnella and reticulum) and external dehiscence like slime mold sporocarps (Stephenson and Stempin, 1994). Podetia and scyphi of lichenized ascomycotans such as *Cladonia ecmocyna* (Fig. 12B and C) have a hollow interior (podetium), terminal cups (scyphus), basal hollow tube (stolon) and indeterminate growth (Fig. 8), but are at least twice the size of *Diskagma*. No convincing lichen reproductive structures (Brodo et al., 2001) have been found in *Diskagma*. Fruiting bodies of basidiomycotan fungi (such as *Phallus impudicus*: Bon, 1987) are also hollow, but are much larger and more ephemeral structures than likely for *Diskagma*. Bladders of the glomeromycotan *Geosiphon pyriformis* have a large internal cavity for cyanobacterial endosymbionts (Schüßler and Kluge, 2000), comparable in size with the inclusion-free central hollow of *Diskagma*, but lack a terminal cup. Fungal affinities of *Diskagma* and *Thucomyces* will remain insecure until definitive reproductive structures are discovered, and also run foul of molecular clocks dating fungi only as far back as 1.1 Ga (Blair, 2009; Berbee and Taylor, 2010a,b).

7. Conclusions

Thucomyces (2.8 Ga) and *Diskagma* (2.2 Ga) are locally abundant fossils at the surface of paleosols (Retallack, 1986; Mossman et al., 2008), and thus evidence of life on land. They demonstrate the megascopic appearance of life on Neoproterozoic and Paleoproterozoic landscapes. They also provide search images for more conclusive evidence of Archean and Proterozoic life on land, preferably in paleosols permineralized in ways comparable with marine cherts (Schopf et al., 2010) or compressed in organic seams (thucolites: Mossman et al., 2008).

Unfortunately, sexual reproductive structures are unknown and exact biological affinities are thus uncertain for both *Diskagma* and *Thucomyces*. Irregular internal partitions and even floor and roof levels of *Thucomyces* are like columnar bacterial biofilms (Hall-Stoodley et al., 2004), but poorly known actinobacterial symbioses are also a plausible alternative (Kalakoutskii et al., 1990). With its urn shape, basal stolon and complex apical cup, *Diskagma* is a promising candidate for the oldest known eukaryote, perhaps an endocyanotic glomeromycotan like living *Geosiphon* (Fig. 12D). Previously known fungi and actinobacteria are 1.5 Ga endocyanotic Glomeromycota (Retallack et al., 2013), 0.6 Ga lichenized Glomeromycota (Yuan et al., 2005), 0.6 Ga parasitic actinobacteria (Gnilovskaya, 1985), and 0.4 Ma parasitic Ascomycota (Sherwood-Pike and Gray, 1985; Taylor et al., 1999, 2004). Other possible eukaryotes considered marine include 2.1 Ga Franceville fossils (El Albani et al., 2010), 1.9 Ga siphonous alga *Grypania* (Han and Runnegar, 1992; Schneider et al., 2002), and 1.8 Ga Panjiapu acritarchs (Lambe et al., 2009). Molecular clocks remain at odds with interpretation of some of these fossils, because they place the origin of Actinobacteria at 2.7 Ga (Battistuzzi and Hedges, 2009), Eukaryota at 1.6 Ga (Bhattacharya et al., 2009) and Fungi at 1.1 Ga (Blair, 2009; Berbee and Taylor, 2010a,b). Taking a hardline molecular clock approach, Franceville fossils, *Thucomyces*, *Diskagma*, *Grypania* and Panjiapu acritarchs would all be prokaryotes, perhaps actinobacteria (Cavalier-Smith, 2006). A second hypothesis supported by Han and Runnegar (1992) and Knoll et al. (2006) is that *Grypania* marks the origin of eukaryotes, in which case Franceville fossils, *Diskagma* and *Thucomyces* would have been unusually elaborate prokaryotes. Complexity of *Diskagma* in paleosols reported here is comparable or greater than the modern Glomeromycotan *Geosiphon*, both a fungus and a terrestrial eukaryote, and opens a third hypothesis, that eukaryotes and fungi on land date back to 2.2 Ga. Two corollaries of this third hypothesis, should it resist falsification, are (1) that molecular clocks should be recalibrated, and (2) that fungi evolved on land earlier than in the sea. *Diskagma* and *Thucomyces* in paleosols provide search images for discovery of additional fossils preserved adequately to test these hypotheses.

Acknowledgments

We thank Whitey Hagadorn, Richard Ketchum, and Bill Carlson for help with early attempts at X-ray microtomography, and Michael Schaffer for help with the electron microprobe. Alastair MacDowell and Casey Abernathy helped with synchrotron X-ray microtomography. Dick Holland, Hiroshi Ohmoto, Bruce Runnegar, Stefan Bengtson, Paul Strother, Mihail Tomescu, Nathan Sheldon, and Dima Grazhdankin offered helpful discussions.

References

- Allwood, A.C., Walter, M.R., Kamber, B.S., Marshall, C.P., Burch, I.W., 2006. Stromatolite reef from the Early Archaean era of Australia. *Nature* 441, 714–718.
- Andrews, L.M., Railsback, L.B., 1997. Controls on stylonite development: morphologic, lithologic, and temporal evidence from bedding-parallel and transverse stylonites from the U.S. Appalachians. *Journal of Geology* 105, 59–73.

- Barghoorn, E.S., 1981. Aspects of Precambrian paleobiology. In: Niklas, K.J. (Ed.), *Paleobotany, paleoecology and evolution*, 1. Praeger, New York, pp. 1–16.
- Barnicoat, A.C., Henderson, L.H.C., Knipe, R.J., Yardley, B.W.D., Napier, R.W., Fox, N.P.C., Kenyon, A.K., Muntigh, D.J., Styrdom, D., Winker, K.S., Lawrence, S.R., Cornford, C., 1997. Hydrothermal gold mineralization in the Witwatersrand Basin. *Nature* 386, 820–824.
- Basile, A., Sorbo, S., Aprile, G., Conte, B., Cobiانchi, R.C., 2008. Comparison of the heavy metal bioaccumulation capacity of an epiphytic moss and an epiphytic lichen. *Environmental Pollution* 151, 401–407.
- Bhattacharya, D., Soon, H.S., Hedges, S.B., Hackett, J.D., 2009. Eukaryotes (Eukaryota). In: Hedges, S.B., Kumar, S. (Eds.), *The Timetree of Life*. Oxford Univ. Press, New York, pp. 116–120.
- Battistuzzi, F.U., Hedges, S.B., 2009. A major clade of prokaryotes with ancient adaptations to land. *Molecular Biology and Evolution* 26, 335–343.
- Berbee, M.L., Taylor, J.W., 2010a. Dating the molecular clock in fungi—how close are we? *Fungal Biology Reviews* 24, 1–16.
- Bekker, A., Holland, H.D., 2012. Oxygen overshoot and recovery during the early Paleoproterozoic. *Earth and Planetary Science Letters* 317–318, 295–304.
- Bekker, A., Kaufman, A.J., Karhu, J.A., Eriksson, K.A., 2005. Evidence for Paleoproterozoic cap carbonates in North America. *Precambrian Research* 137, 167–206.
- Berbee, M.L., Taylor, J.W., 2010b. Dating the molecular clock in fungi – how close are we? *Fungal Biology Reviews* 24, 1–16.
- Beukes, N.J., Dorland, H., Gutzmer, J., Nedachi, M., Ohmoto, H., 2002. Tropical laterites, life on land, and the history of atmospheric oxygen in the Paleoproterozoic. *Geology* 30, 491–494.
- Bever, J.D., Wang, M., 2005. Arbuscular mycorrhizal fungi: hyphal fusion and multigenomic structure. *Nature* 433, E3–E4.
- Blair, J.E., 2009. Fungi. In: Hedges, S.B., Kumar, S. (Eds.), *The Timetree of Life*. Oxford Univ. Press, New York, pp. 215–219.
- Bon, M., 1987. *The Mushrooms and Toadstools of Britain and North-Western Europe*. Hodder and Stoughton, London.
- Brimhall, G.H., Chadwick, O.A., Lewis, C.J., Compston, W., Williams, I.S., Danti, K.J., Dietrich, W.E., Power, M.E., Hendricks, D., Bratt, J., 1992. Deformational mass transport and invasive processes in soil evolution. *Science* 255, 695–702.
- Brodo, I.M., Sharnoff, S.D., Sharnoff, S., 2001. *Lichens of North America*. Yale Univ. Press, New Haven.
- Buchanan, P.C., Reimold, W.U., Koerber, C., Kruger, F.J., 2004. Rb/Sr and Sm/Nd isotopic compositions of the Rooiberg Group, South Africa; early Bushveld-related volcanism. *Lithos* 75, 373–388.
- Buick, I.S., Maas, R., Gibson, R., 2001. Precise U–Pb titanite age constraints on the emplacement of the Bushveld Complex, South Africa. *Journal of the Geological Society of London* 158, 3–6.
- Butterfield, N.J., 2005. Probable Proterozoic fungi. *Paleobiology* 31, 165–182.
- Button, A., 1975. A palaeocurrent study of the Dwaal Heuvel Formation, Transvaal Group. *Geological Society of South Africa Transactions* 78, 173–183.
- Button, A., 1979. Early Proterozoic weathering profile on the 2200 m.y. old Hekpoort Basalt, Pretoria Group, South Africa: preliminary results. *Information Circular – University of the Witwatersrand, Economic Geology Research Unit* 133, 1–29.
- Button, A., Tyler, N., 1981. The character and economic significance of Precambrian paleoweathering and erosion surfaces in southern Africa. *Economic Geology Anniversary Issue for 1981*, 686–709.
- Cashman, K.V., Kauahikaua, J.P., 1997. Reevaluation of vesicle distributions in basalt flows. *Geology* 25, 419–422.
- Cavalier-Smith, T., 2006. Cell evolution and Earth history: stasis and revolution. *Philosophical Transactions of the Royal Society of London* 361, 969–1006.
- Clites, E.C., Droser, E.L., Gehling, J.G., 2012. The advent of hard-part structural support among the Ediacara biota: ediacaran harbinger of a Cambrian mode of body construction. *Geology* 40, 307–310.
- Cloud, P.E., 1976. The beginnings of biospheric evolution and their biochemical consequences. *Paleobiology* 2, 351–387.
- Cohen, P.A., Knoll, A.H., Kodner, R.B., 2009. Large spinose microfossils in Ediacaran rocks as resting stages of early animals. *Proceedings of the National Academy of Sciences of the United States of America* 106, 6519–6524.
- Cornell, D.H., Schütte, S.S., Eglinton, B.L., 1996. The Ongeluk basaltic andesite formation in Griqualand West, South Africa: submarine alteration in a 2222 Ma Proterozoic sea. *Precambrian Research* 79, 101–123.
- de la Rosa, J.P.M., Warke, P.A., Smith, B.J., 2012. Microscale biopitting by the endolithic lichen *Verrucaria baldensis* and its proposed role in mesoscale solution basin development on limestone. *Earth Surface Processes and Landforms* 37, 374–384.
- Delvigne, J.E., 1998. Atlas of micromorphology of mineral alteration and weathering. *Canadian Mineralogist Special Publication* 3, 1–493.
- Dorn, R.L., Oberlander, T.M., 1982. Rock varnish. *Progress in Physical Geography* 6, 317–367.
- Driese, S.G., 2004. Pedogenic translocation of Fe in modern and ancient Vertisols and implications for interpretations of the Hekpoort Paleosol (2.25 Ga). *Journal of Geology* 112, 543–560.
- Driese, S.G., Mora, C.I., Cotter, E., Foreman, J.L., 1992. Paleopedology and stable isotope chemistry of Late Silurian vertic paleosols, Bloomsburg Formation, central Pennsylvania. *Journal of Sedimentary Petrology* 62, 825–841.
- Droser, M.L., Gehling, J.G., 2008. Synchronous aggregate growth in an abundant new Ediacaran tubular organism. *Science* 319, 1660–1662.
- Dunne, W.M., 2002. Bacterial adhesion: seen any good biofilms lately? *Clinical Microbiology Reviews* 15, 155–166.
- El Albani, A., Bengtson, S., Canfield, D.E., Bekker, A., Macchiarelli, R., Arnaud Mazurier, A., Hammarlund, E.U., Boulvais, P., Dupuy, J.-J., Fontaine, C., Fürsich, F.T., Gauthier-Lafaye, F., Janvier, P., Javaux, E., Ossa, F.O., Pierson-Wickmann, A.-C., Riboulleau, A., Sardini, P., Vachard, D., Whitehouse, M., Meunier, A., 2010. Large colonial organisms with coordinated growth in oxygenated environments 2.1 Gyr ago. *Nature* 466, 100–104.
- Ernst, R.E., Buchan, K.L., 2002. Maximum size and distribution in time and space of mantle plumes: evidence from large igneous provinces. *Journal of Geodynamics* 34, 309–342.
- Farquhar, J., Wing, B.A., 2003. Multiple sulfur isotopes and the evolution of the atmosphere. *Earth and Planetary Science Letters* 213, 1–13.
- Fletcher, B.J., Beerling, D.J., Chaloner, W.G., 2004. Stable carbon isotopes and the metabolism of the terrestrial Devonian organism *Spongiophyton*. *Geobiology* 2, 107–119.
- Frey, S.E., Gingras, M.K., Dashtgard, S.E., 2009. Experimental studies of gas-escape and water escape structures: mechanisms and morphologies. *Journal of Sedimentary Research* 79, 808–816.
- Gnilovskaya, M.B., 1985. Vendian actinomycetes and organisms of uncertain systematic position. In: Sokolov, B.S., Iwanowski, A.B. (Eds.), *The Vendian System: v.1 Paleontology*. Springer, Berlin, pp. 148–153.
- Grey, K., Yochelson, E.L., Fedonkin, M.A., Martin, D.M., 2010. *Horodyskia williamsi*, new species, a Mesoproterozoic fossil from Western Australia. *Precambrian Research* 180, 1–17.
- Grotzinger, J.P., Watters, W.A., Knoll, A.H., 2000. Calcified metazoans in thrombolite-stromatolite reefs of the terminal Proterozoic Nama Group, Namibia. *Paleobiology* 26, 334–359.
- Grové, D., Harris, C., 2010. O- and H-isotope study of the Carbon Leader Reef at the Tau Tona and Savuka Mines (Western Deep Levels), South Africa; implications for the origin and evolution of Witwatersrand Basin fluids. *South African Journal of Geology* 113, 73–86.
- Hall-Stoodley, L., Costerton, J.W., Stoodley, P., 2004. Bacterial biofilms: from the natural environment to infectious diseases. *Nature Reviews Microbiology* 2, 95–108.
- Hallbauer, D.K., van Warmelo, K.T., 1974. Fossilized plants in thucolite from the Witwatersrand, South Africa. *Precambrian Geology* 1, 199–212.
- Hallbauer, D.K., Jahns, M.H., Beltmann, H.A., 1977. Morphological observations on some Precambrian plants from the Witwatersrand, South Africa. *Geologische Rundschau* 66, 477–491.
- Han, T.-M., Runnegar, B., 1992. Megascopic eukaryotic algae from the 2.1-billion-year-old Negaunee Iron-Formation. *Science* 257, 232–235.
- Hannah, J.L., Stein, H.J., Bekker, A., Wilkinson, J.J., Beukes, N.J., van Niekerk, H.S., 2004. Primitive Os and 2,316 Ma age for marine shale: implications for Paleoproterozoic glacial events and the rise of atmospheric oxygen. *Earth and Planetary Science Letters* 225, 43–52.
- Hobbie, E.A., Boyce, C.K., 2010. Carbon sources for the Palaeozoic giant fungus *Prototaxites* inferred from modern analogues. *Proceedings of the Royal Society of London B* 277, 2149–2156.
- Hoefs, J., Schidlowski, M., 1967. Carbon isotope composition of carbonaceous matter from the Precambrian of the Witwatersrand. *Science* 155, 1096–1097.
- Hoffman, H.J., 2004. Archean microfossils and abiomorphs. *Astrobiology* 4, 35–36.
- Holland, H.D., 1984. *The Chemical Evolution of the Atmosphere and Oceans*. Princeton Univ. Press, Princeton.
- Holland, H.D., Beukes, N.J., 1990. A paleoweathering profile from Griqualand West, South Africa: evidence for a dramatic rise in atmospheric oxygen between 2.2 and 1.9 byk. *American Journal of Science* 289, 362–389.
- Holland, H.D., Rye, R., Ohmoto, H., 1997. Evidence in pre-2.2 Ga paleosols for the early evolution of atmospheric oxygen and terrestrial biota—discussion and reply. *Geology* 25, 857–858.
- Jahren, A.H., Porter, S., Kuglitsch, J.J., 2003. Lichen metabolism identified in Early Devonian terrestrial organisms. *Geology* 31, 99–102.
- Javaux, E.J., Knoll, A.H., Walter, M.R., 2001. Morphological and ecological complexity in early eukaryotic ecosystems. *Nature* 412, 66–69.
- Javaux, E.J., Marshall, C.P., Bekker, A., 2010. Organic-walled microfossils in 3.2-billion-year-old shallow marine siliciclastic deposits. *Nature* 463, 934–938.
- Jones, D.S., Maloof, A.C., Hurtgen, M.T., Rainbird, R.H., Schrag, D.P., 2010. Regional and global chemostratigraphic correlation of the early Neoproterozoic Shaler Supergroup, Victoria Island, northwestern Canada. *Precambrian Research* 181, 43–63.
- Kalakoutskii, L.V., Zenova, G.M., Soina, V.S., Likhacheva, A.A., 1990. Associations of actinomycetes with algae. *Actinomycetes* 1, 27–42.
- Kasting, J.F., Catling, D., 2003. Evolution of a habitable planet. *Annual Review of Astronomy and Astrophysics* 41, 429–463.
- Kauffman, E.G., Steidtmann, J.R., 1981. Are these the oldest metazoan trace fossils? *Journal of Paleontology* 55, 923–947.
- Kent, L.E. (Ed.), 1980. *Stratigraphy of South Africa*. *Geol. Surv. South Africa Handbk* 8, pp. 1–690.
- Knoll, A.H., 2003. *Life on a Young Planet: The First Three Billion Years of Evolution on Earth*. Princeton Univ. Press, Princeton.
- Knoll, A.H., Javaux, E.J., Hewitt, D., Cohen, P., 2006. Eukaryotic organisms in Proterozoic oceans. *Philosophical Transactions of the Royal Society of London* 361, 1023–1038.
- Kopp, R.E., Kirschvink, J.L., Hilburn, I.A., Nash, C.Z., 2005. The Paleoproterozoic snowball Earth: a climate disaster triggered by the evolution of oxygenic photosynthesis. *Proceedings of the National Academy of Sciences of the United States of America* 102, 11131–11136.

- Lamb, D.M., Awramik, S.M., Chapman, D.J., Zhu, S., 2009. Evidence for eukaryotic diversification in the ~1800 million-year-old Changzhougou Formation, North China. *Precambrian Research* 173, 93–104.
- Luoma, S.N., Rainbow, P.S., 2006. Why is metal bioaccumulation so variable? Biodynamics as a unifying concept. *Environmental Science and Technology* 39, 1921–1931.
- Macfarlane, A.W., Holland, H.D., 1991. The timing of alkali metasomatism in palaeosols. *Canadian Mineralogist* 29, 1043–1050.
- MacRae, C., 1999. Life Etched in Stone. Geol. Soc., Johannesburg, South Africa.
- Mapeo, R.B.M., Armstrong, R.A., Kampunzu, A.B., Modisi, M.P., Ramokate, L.V., Modie, B.N.J., 2006. A ca. 200 Ma hiatus between the Lower and Upper Transvaal Groups of southern Africa: SHRIMP U–Pb detrital zircon evidence from the Segwagwa Group, Botswana: implications for Palaeoproterozoic glaciations. *Earth and Planetary Science Letters* 244, 113–132.
- Maynard, J.B., 1992. Chemistry of modern soils as a guide to interpreting Precambrian paleosols. *Journal of Geology* 100, 279–289.
- McFadden, L.D., McDonald, E.V., Wells, S.G., Anderson, K., Quade, J., Forman, S.L., 1998. The vesicular layer and carbonate collars of desert soils and pavements: formation, age and relation to climate change. *Geomorphology* 24, 101–145.
- McNeill, J., Barrie, F.R., Burdet, H.M., Demoulin, V., Hawksworth, D.L., Marhold, K., Nicolson, D.H., Prado, J., Silva, P.C., Skog, J.E., Wiersma, J.H., Turland, N.J. (Eds.), 2006. International code of botanical nomenclature (Vienna Code) adopted by the seventeenth International Botanical Congress, Vienna. *Ganter, Königstein*.
- Moczyłowska, M., Landing, E., Zang, W., Palacios, T.T., 2011. Proterozoic phytoplankton and the timing of chlorophyte algae origins. *Palaeontology* 54, 721–733.
- Mossman, D.J., Minter, W.E.L., Dutkiewicz, A., Hallbauer, D.K., George, S.C., Hennigh, Q., Reimer, T.O., Horscroft, F.D., 2008. The indigenous origin of Witwatersrand carbon. *Precambrian Research* 164, 173–186.
- Murakami, T., Sreenivas, B., Sharma, S.D., Sugimori, H., 2011. Quantification of atmospheric oxygen levels during the Paleoproterozoic using paleosol compositions and iron oxidation kinetics. *Geochimica et Cosmochimica Acta* 75, 3982–4004.
- Nagy, B., Nagy, L.A., Rigali, M.J., Jones, W.D., Krinsley, D.H., Sinclair, N.A., 1991. Rock varnish in the Sonoran Desert: microbiologically mediated accumulation of manganese-rich sediments. *Sedimentology* 38, 1153–1171.
- Neaman, A., Chorover, J., Brantley, S.L., 2005. Element mobility patterns record organic ligands in soils on early Earth. *Geology* 33, 117–120.
- Oberholzer, J.D., Eriksson, P.G., 2000. Subaerial volcanism in the Palaeoproterozoic Hekpoort Formation (Transvaal Supergroup), Kaapvaal Craton. *Precambrian Research* 101, 193–210.
- Ohmoto, H., 1996. Evidence in pre-2.2 Ga paleosols for the early evolution of atmospheric oxygen and terrestrial biota. *Geology* 24, 1135–1138.
- Palmer, J.A., Phillips, F.N., McCarthy, T.S., 1989. Paleosols and their relevance to Precambrian atmospheric composition. *Journal of Geology* 97, 77–92.
- Pellegrin, V., Juretschko, S., Wagner, M., Cottenceau, G., 1999. Morphological and biochemical properties of a *Sphaerotilus* sp. isolated from paper mill slimes. *Applied and Environmental Microbiology* 65, 156–162.
- Porter, S.M., Meisterfeld, R., Knoll, A.H., 2003. Vase-shaped microfossils from the Neoproterozoic Chuar Group, Grand Canyon. *Journal of Paleontology* 77, 409–429.
- Potter, S.L., Chan, M.A., Peterson, E.U., Dyar, M.D., Sklute, E., 2011. Characterization of Navajo Sandstone concretions: mars comparison and criteria for establishing diagenetic origins. *Earth and Planetary Science Letters* 301, 444–456.
- Prashnowsky, A.A., Schidlowski, M., 1967. Investigation of a Precambrian thucolite. *Nature* 216, 560–563.
- Rahmatullah, Dixon, J.B., Bowman, J.R., 1990. Manganese-containing nodules in two calcareous rice soils of Pakistan. In: Douglas, L.A. (Ed.), *Soil Micromorphology: A Basic and Applied Science*. Elsevier, Amsterdam, pp. 387–394.
- Rainbow, P.S., 2006. Trace metal bioaccumulation: models, metabolic availability and toxicity. *Environment International* 33, 576–658.
- Retallack, G.J., 1986. Reappraisal of a 2200-Ma-old paleosol from near Waterval Onder, South Africa. *Precambrian Research* 32, 195–252.
- Retallack, G.J., 1989. Paleosols and their relevance to Precambrian atmospheric composition: comment. *Journal of Geology* 97, 763–764.
- Retallack, G.J., 1991. Untangling the effects of burial alteration and ancient soil formation. *Annual Review of Earth and Planetary Sciences* 19, 183–206.
- Retallack, G.J., 1997. A Colour Guide to Paleosols. John Wiley & Sons, Chichester.
- Retallack, G.J., 2007. Decay, growth, and burial compaction of *Dickinsonia*, an iconic Ediacaran fossil. *Alcheringa* 31, 215–240.
- Retallack, G.J., 2009. Refining a pedogenic CO₂ paleobarometer for quantifying the middle Miocene greenhouse spike. *Palaeogeography, Palaeoclimatology, Palaeoecology* 281, 57–65.
- Retallack, G.J., 2010. Lateritization and bauxitization events. *Economic Geology* 105, 655–667.
- Retallack, G.J., 2011. Problematic megafossils in Cambrian palaeosols of South Australia. *Palaeontology* 54, 1223–1242.
- Retallack, G.J., 2013a. A short history and long future of paleopedology. In: Driese, S.G. (Ed.), *New Frontiers in Paleopedology and Terrestrial Paleoclimatology*. Soc. Econ. Paleont. Mineral. Spec. Pap. 44, pp. 5–16.
- Retallack, G.J., 2013b. Permian and Triassic greenhouse crises. *Gondwana Research* 24, 90–103.
- Retallack, G.J., Dilcher, D.L., 2012. Core and geophysical logs versus outcrop for interpretation of Cretaceous paleosols in the Dakota Formation of Kansas. *Palaeogeogr. Palaeoclim. Paleoc 329–330*, 47–63.
- Retallack, G.J., Krinsley, D.H., 1993. Metamorphic alteration of a Precambrian (2.2 Ga) paleosol from South Africa. *Precambrian Res* 63, 27–41.
- Retallack, G.J., Bestland, E.A., Fremd, T.J., 2000. Eocene and Oligocene paleosols of central Oregon. Special Paper – Geological Society of America 344, 1–192.
- Retallack, G.J., Dunn, K.L., Saxby, J., 2013. Problematic Mesoproterozoic fossil *Horodyskia* from Glacier National Park, Montana, USA. *Precambrian Research* 226, 125–142.
- Rhodes, B.P., Conejo, R., Benchawan, T., Titus, S., Lawson, R., 2005. Palaeocurrents and provenance of the Mae Rim Formation, northern Thailand: implications for the tectonic evolution of the Chiang Mai Basin. *Journal of the Geological Society of London* 162, 51–63.
- Rye, R., Holland, H.D., 2000a. Geology and geochemistry of paleosols developed on the Hekpoort Basalt, Pretoria Group, South Africa. *American Journal of Science* 300, 85–141.
- Rye, R., Holland, H.D., 2000b. Erratum; geology and geochemistry of paleosols developed on the Hekpoort Basalt, Pretoria Group, South Africa. *American Journal of Science* 300, 344–345.
- Sawidis, T., Chettri, M.K., Zachariadis, G.A., Stratis, J.A., Seaward, M.R.D., 1995. Heavy metal bioaccumulation in lichens from Macedonia in northern Greece. *Toxicological and Environmental Chemistry* 50, 157–166.
- Schaefer, B.F., Pearson, D.G., Rogers, N.W., Barnicoat, A.C., 2010. Re/Os isotope and PGE constraints on the timing and origin of gold mineralisation in the Witwatersrand Basin. *Chemical Geology* 276, 88–94.
- Schidlowski, M., Hayes, J.M., Kaplan, I.R., 1983. Isotopic inferences of ancient biochemistries: carbon, sulfur, hydrogen and nitrogen. In: Schopf, J.W. (Ed.), *Earth's Earliest Biosphere*. Princeton Univ. Press, Princeton, pp. 149–186.
- Schneider, D.A., Bickford, M.E., Cannon, W.F., Schulz, K.J., Hamilton, M.A., 2002. Age of volcanic rocks and syndepositional iron formations, Marquette Range Supergroup: implications for the tectonic setting of Paleoproterozoic iron formations of the Lake Superior region. *Canadian Journal of Earth Sciences* 39, 999–1012.
- Schopf, J.W., Klein, C. (Eds.), 1991. *The Proterozoic Biosphere: A Multidisciplinary Study*. Cambridge Univ. Press, Cambridge.
- Schopf, J.W., Kudryavtsev, A.B., Sugitani, K., Walter, M.R., 2010. Precambrian microbe-like pseudofossils: a promising solution to the problem. *Precamb. Res* 179, 191–205.
- Schüßler, A., Kluge, M., 2000. *Geosiphon pyriformis*, an endocytosymbiosis between fungus and cyanobacteria, and its meaning as a model system for arbuscular mycorrhizal research. In: Hock, B. (Ed.), *The Mycota IX*. Springer, Berlin, pp. 151–161.
- Sheldon, N.D., 2006. Precambrian paleosols and atmospheric CO₂ levels. *Precamb. Res* 147, 148–155.
- Sheldon, N.D., Retallack, G.J., 2001. Equation for compaction of paleosols due to burial. *Geology* 29, 247–250.
- Sheldon, N.D., Retallack, G.J., Tanaka, S., 2002. Geochemical climofunctions from North American soils and application to paleosols across the Eocene-Oligocene boundary in Oregon. *Journal of Geology* 110, 687–696.
- Sherwood-Pike, M.A., Gray, J., 1985. Silurian fungal remains: probable records of the Class Ascomycetes. *Lethaia* 18, 1–20.
- Som, S.M., Catling, D.C., Harnmeijer, J.P., Polivka, P.M., Buick, R., 2012. Air density 2.7 billion years ago limited to less than twice modern levels by fossil raindrop imprints. *Nature* 484, 360–362.
- Spicer, R.A., 1977. The pre-depositional formation of some leaf impressions. *Palaeontology* 20, 907–912.
- Staley, J.T., Palmer, F., Adams, J.B., 1982. Microcolonial fungi: common inhabitants on desert rocks? *Science* 215, 1093–1095.
- Stephenson, S.L., Stempen, H.H., 1994. *Myxomycetes: A Handbook of Slime Molds*. Timber Press, Portland.
- Strother, P.K., Battison, L., Brasier, M.D., Wellman, C.H., 2011. Earth's earliest non-marine eukaryotes. *Nature* 473, 505–509.
- Sugitani, K., Grey, K., Hagaoka, T., Mimura, K., 2009. Three-dimensional morphological and textural complexity of Archaeal putative microfossils from the northeastern Pilbara craton: indications of large (>15 μm) spheroidal and spindle-like structures. *Astrobiology* 9, 603–615.
- Suthar, S., Singh, S., Dhawan, S., 2008. Earthworms as bioindicator of metals (Zn, Fe, Mn, Cu, Pb and Cd) in soils: is metal bioaccumulation affected by their ecological category? *Ecological Engineer* 32, 99–107.
- Taylor, T.N., Hass, T., Kerp, H., 1999. The oldest fossil ascomycetes. *Nature* 399, 648.
- Taylor, T.N., Hass, H., Kerp, H., Krings, M., Hanlin, R.T., 2004. Perithecial ascomycetes from the 400 million year old Rhyne chert: an example of ancestral polymorphism. *Mycologia* 96, 1403–1419.
- Tomescu, A.M.F., Pratt, L.M., Rothwell, G.W., Strother, P.K., Nadon, G.C., 2009. Carbon isotopes support the presence of extensive land floras pre-dating the origin of vascular plants. *Palaeogeogr. Palaeoclim. Paleoc 283*, 46–59.
- van Kranendonk, M.J., Philpott, P., Lepot, K., Bodorkos, S., Pirajno, F., 2008. Geological setting of the Earth's oldest fossils in the ca. 3.5 Ga Dresser Formation, Pilbara Craton, Western Australia. *Precambrian Research* 167, 93–124.
- van Veen, W.L., Mulder, E.G., Deinema, M.H., 1978. The *Sphaerotilus leptothrix* group of bacteria. *Microbiol. Rev* 42, 239–356.
- Wacey, D., Kilburn, M.R., Saunders, M., Cliff, J., Brasier, M.D., 2011. Microfossils of sulfur-metabolizing cells in 3.4-billion-year-old rocks of Western Australia. *Nature Geoscience* 4, 698–702.
- Walraven, F., 1997. Geochronology of the Rooiberg Group, Transvaal Supergroup, South Africa. Information Circular – University of the Witwatersrand, Economic Geology Research Unit 316, 1–21.

- Watanabe, Y., Stewart, B.W., Ohmoto, H., 2004. Organic- and carbonate-rich soil formation approximately 2.6 billion years ago at Schagen, east Transvaal District, South Africa. *Geochimica et Cosmochimica Acta* 68, 2129–2151.
- Wiggering, H., Beukes, N.J., 1990. Petrography and geochemistry of a 2000–2200-Ma-old hematitic paleo-alteration profile on Ongeluk Basalt of the Transvaal Supergroup, Griqualand West, South Africa. *Precambrian Research* 46, 241–258.
- Wordsworth, R., Pierrehumbert, R., 2013. Hydrogen-nitrogen greenhouse warming in Earth's early atmosphere. *Science* 339, 64–67.
- Yamaguchi, K.E., Johnson, C.M., Beard, B.L., Beukes, N.J., Gutzmer, J., Ohmoto, H., 2007. Isotopic evidence for iron mobilization during Paleoproterozoic lateritization of the Hekpoort palaeosol profile from Gaborone, Botswana. *Earth and Planetary Science Letters* 256, 577–587.
- Yang, W., Holland, H.D.H.D., 2003. The Hekpoort Paleosol profile in Strata 1 at Gaborone, Botswana; soil formation during the great oxidation event. *American Journal of Science* 303, 187–220.
- Yuan, X., Xiao, S., Taylor, T.N., 2005. Lichen-like symbiosis 600 million years ago. *Science* 308, 1017–1020.